MASTERARBEIT | MASTER'S THESIS

Titel | Title

Metabolic Adaptations to Different Dietary Interventions: Gene Expression Analysis in Murine Liver and Heart

verfasst von | submitted by

Janina Melanie Kliewe

angestrebter akademischer Grad | in partial fulfilment of the requirements for the degree of

Master of Science (MSc)

Wien | Vienna, 2026

Studienkennzahl lt. Studienblatt | Degree programme code as it appears on the student record sheet:	UA 066 838
Studienrichtung lt. Studienblatt | Degree programme as it appears on the student record sheet:	Masterstudium Ernährungswissenschaften
Betreut von | Supervisor:	Univ.-Prof. Dr. Jürgen König
Mitbetreut von | Co-Supervisor:	Dr. Felix Sternberg B.rer.nat. MSc

Table of Content

0. Abstract

Ketogene Diäten (KD) haben sich weit über ihre Ursprünge in der Epilepsietherapie hinaus entwickelt und werden heute als metabolische Intervention bei Adipositas, kardiovaskulären Erkrankungen und Neurodegeneration untersucht. Ihr wesentliches Merkmal ist dabei nicht allein ein hoher Fettgehalt, sondern eine starke Reduktion der Kohlenhydratzufuhr, die den Stoffwechsel von Glukoseoxidation zur Fettsäureoxidation (FAO) und hepatischen Ketonkörper-Produktion verschiebt. Doch nicht alle Nahrungsfette werden gleich metabolisiert. Mittelkettige Triglyceride (MCT) und langkettige Triglyceride (LCT) unterscheiden sich grundlegend in ihrer Absorption, hepatischen Verarbeitung und oxidativen Verwertung. Ob diese Unterschiede die Genexpression auf gewebespezifische Weise prägen, ist bisher noch unvollständig verstanden.

Die vorliegende Studie untersuchte, wie verschiedene Ernährungsinterventionen die transkriptionelle Regulation des Lipidstoffwechsels, der mitochondrialen Dynamik und der zellulären Stressantwort in zwei metabolisch unterschiedlichen Organen, der Leber und dem Herzen, beeinflussen. Männliche C57BL/6NRJ-Mäuse wurden randomisiert einer von fünf Ernährungsgruppen zugeteilt: einer LCT-angereicherten KD, einer kombinierten LCT/MCT-KD, Kalorienrestriktion (CR), intermittierendem Fasten (IF) oder einer Standarddiät (SD) als Referenzdiät. Die Intervention erstreckte sich über acht Wochen, wobei CR und IF in den letzten zwei Wochen eingeführt wurden. Die Genexpression wurde mittels RT-qPCR in Herz- und Lebergewebe quantifiziert.

Die Leber erwies sich als das transkriptionell reaktionsfreudigere Organ. KD, insbesondere die LCT-Diät, reduzierten die Expression lipogener Gene und steigerten gleichzeitig die Kapazität zur FAO. Die Anwesenheit von MCTs dämpfte diese Reaktion. Das Herz zeigte demgegenüber deutlich moderatere transkriptionelle Veränderungen, insbesondere unter ketogenen Bedingungen, was auf eine stärkere Abhängigkeit von post-translationalen Regulationsmechanismen hindeuten könnte. Gene der mitochondrialen Dynamik blieben in beiden Geweben weitgehend stabil, während Energierestriktion selektiv stressbezogene Transkriptionsprogramme reduzierte.

Abstract

Ketogenic diets (KD) have moved far beyond their origins in epilepsy treatment. Today they are investigated as metabolic interventions for obesity, cardiovascular disease and neurodegeneration. Their defining feature is not simply fat abundance, but a pronounced restriction of dietary carbohydrates, shifting metabolism away from glucose oxidation toward fatty acid oxidation (FAO) and hepatic ketone body production. Yet not all dietary fats are metabolized equally. Medium-chain triglycerides (MCT) and long-chain triglycerides (LCT) differ fundamentally in their absorption, hepatic handling and oxidative fate. However, whether this shapes gene expression in a tissue-specific manner remains incompletely understood.

This study examined how distinct dietary interventions influence the transcriptional regulation of lipid metabolism, mitochondrial dynamics and cellular stress signaling in two metabolically distinct organs, the liver and the heart. Male C57BL/6NRJ mice were randomly assigned to one of five dietary groups: an LCT-enriched KD, a combined LCT/MCT KD, calorie restriction (CR), intermittent fasting (IF) or a standard diet (SD) as a reference condition. The intervention period lasted eight weeks, with CR and IF introduced only during the final two weeks. Gene expression was quantified by RT-qPCR in cardiac and hepatic tissue. The liver appeared as the more transcriptionally responsive organ: KDs, particularly the LCT diet, suppressed lipogenic gene expression while upregulating FAO capacity. The presence of MCTs attenuated this response. The heart, by contrast, showed more modest transcriptional changes across dietary conditions, especially regarding KDs, suggesting a greater reliance on post-translational regulatory mechanism. Genes governing mitochondrial dynamics remained largely stable in both tissues, while energy restriction selectively suppressed stress-related transcriptional paths.

1. Introduction

Diet composition influences metabolic homeostasis on multiple levels: Not only through energy supply, but also through modulation of lipid metabolism (Hilary et al., 2024), mitochondrial dynamics (Ngo et al., 2023; Putti et al., 2015) and cellular stress responses (Tan & Norhaizan, 2019). Among dietary interventions, ketogenic diets (KDs) have attracted particular attention for their capacity to redirect substrate utilization away from carbohydrates toward fatty acid oxidation (FAO) and hepatic ketogenesis (Kyriazis et al., 2022).

At the center of this metabolic shift, mitochondria as the primary organelles are responsible for energy-transduction and fatty acid catabolism (Putti et al., 2015). Mitochondrial function depends on the type and availability of metabolic substrates, which are largely determined by diet. Recent studies have highlighted that lipid metabolism and mitochondrial architecture are closely linked, suggesting that changes in mitochondrial morphology reflect adaptive responses to altered nutrient availability (Boone & Lewis, 2024; Y. Li et al., 2023).

1.1 Medium-Chain and Long-Chain Triglycerides

In this context, fatty acid chain length has gained growing scientific attention. Medium-chain triglycerides (MCTs) and long-chain triglycerides (LCTs) differ substantially in terms of digestion, cellular uptake and mitochondrial oxidation (Jandacek, 1994). As the prevalence of metabolic disorders, obesity and neurodegenerative diseases continues to rise, dietary fat composition has come into focus as a modifiable factor influencing metabolic and mitochondrial health (A. Engin, 2017; Valentin-Escalera et al., 2024).

Most dietary fats exist in the form of triglycerides, consisting of three fatty acids esterified to a glycerol backbone. These fatty acids can be saturated, monounsaturated or polyunsaturated (PUFA), each with distinct physical and metabolic properties. Their absorption, metabolism and physiological functions are strongly influenced by carbon chain length (Jadhav & Annapure, 2023). Based on the chain length, dietary triglycerides are broadly classified as MCTs, containing medium-chain fatty acids (MCFAs; C6-C12) or LCTs, composed of long-chain fatty acids (LCFAs; >C12) (Schönfeld & Wojtczak, 2016).

After ingestion, LCTs are hydrolyzed in the small intestine by pancreatic lipases into free LCFAs and monoacylglycerols (Merritt & Julliand, 2013). These products are absorbed

by enterocytes, where they are re-esterified to form new triglycerides. The reassembled LCTs are subsequently packaged into chylomicrons, which bypass the liver via the lymphatic system before eventually entering systemic circulation (Jandacek, 1994; Labarthe et al., 2008). Due to the complexity of this process, LCT digestion is comparatively slow (Jadhav & Annapure, 2023). Once chylomicrons reach peripheral tissues, LCFAs are released by lipoprotein lipases and taken up by cells. Before LCFAs can enter the mitochondrial matrix for β-oxidation, they must be activated to acyl-Coenzyme A (acyl-CoA) by acyl-CoA synthases in the cytosol and subsequently transported into the mitochondrial matrix via the carnitine shuttle, involving carnitine palmitoyltransferase 1 (CPT1), carnitine-acylcarnitine translocase and CPT2 (Labarthe et al., 2008; Shcherbakova et al., 2022). This transport step can be inhibited by malonyl-CoA especially in the postprandial state, thereby suppressing LCFA oxidation and favoring lipid storage or incorporation into structural lipids and lipoproteins (Shcherbakova et al., 2022; You et al., 2008).

MCTs show quite different absorption and metabolic dynamics behavior. Their shorter chain-length make them more water-soluble (Bhavsar & St-Onge, 2016; Jadhav & Annapure, 2023; Papamandjaris et al., 1998). After hydrolysis, MCFAs are absorbed directly into the portal vein and transported to the liver without forming chylomicrons (Bach et al., 1989; Papamandjaris et al., 1998). Hepatic MCFA oxidation occurs largely independently of the carnitine-dependent transport system, allowing β-oxidation even in the fed state, when CPT1-dependent LCFA oxidation is suppressed by malonyl-CoA (Jandacek, 1994; Schönfeld & Wojtczak, 2016). However, it should be noted that this carnitine-independent oxidation is tissue-specific and primarily restricted to the liver. In the heart and skeletal muscle, MCFAs have been shown to require carnitine for mitochondrial entry (Pereyra et al., 2023). The resulting acetyl-CoA from hepatic MCFA oxidation can either enter the tricarboxylic acid (TCA) cycle or serve as a substrate for ketogenesis, producing acetoacetate and β-hydroxybutyrate (β-OHB) (Dikalov et al., 2024; Jandacek, 1994). While MCFAs are considered highly ketogenic, LCFAs can also contribute to ketone body production, particularly during fasting or carbohydrate restriction, when malonyl-CoA levels fall and CPT1-mediated LCFA transport is no longer inhibited (Shcherbakova et al., 2022).

Compared to LCTs, MCTs contain lower amounts of PUFAs, which are prone to lipid peroxidation (Calhoon et al., 2015). MCTs are therefore considered more oxidatively stable and associated with a reduced risk of oxidative stress-related conditions, including

atherosclerosis (Halliwell & Chirico, 1993). LCTs, by contrast, are more prone to oxidative degradation, potentially contributing to cellular damage and inflammation (Calhoon et al., 2015). Beyond their oxidative stability, MCTs have a slightly lower caloric density (8.4 kcal/g vs. 9.2 kcal/g for LCTs) and MCFA intake has been associated with reduced body fat mass and improved insulin sensitivity (Bueno et al., 2015; Schönfeld & Wojtczak, 2016).

Taken together, the rapid hepatic oxidation and lower oxidative vulnerability of MCTs support their potential role in limiting lipid-induced cellular stress and improving metabolic flexibility (Halliwell & Chirico, 1993). To understand the mechanisms behind these differences, it is necessary to consider the mitochondrial processes governing lipid metabolism and energy homeostasis.

1.2 Mitochondrial Function and Lipid Metabolism

Mitochondria are dynamic organelles essential for energy production, lipid metabolism and apoptosis (Y. Li et al., 2023). Maintaining their integrity is therefore essential for metabolic homeostasis (Putti et al., 2015). Mitochondrial quality is regulated through coordinated processes of fusion, fission, mitophagy and biogenesis (Y. Li et al., 2023; Mishra & Chan, 2016).

At the core of mitochondrial function is the regulation of lipid metabolism. Mitochondria are the primary site of FAO, where fatty acids are broken down to acetyl-CoA, which fuels the TCA cycle and drives oxidative phosphorylation via the generation of nicotinamide adenine dinucleotide (NADH) and reduced flavin adenine dinucleotide ($FADH_2$) (Jandacek, 1994; Nolfi-Donegan et al., 2020). Under carbohydrate restriction or fasting, excess acetyl-CoA is redirected toward hepatic ketogenesis (Dikalov et al., 2024). Mitochondria also synthesize structural lipids such as cardiolipin, which is essential for maintaining mitochondrial membrane integrity. Disruptions in mitochondrial lipid metabolism can therefore contribute to insulin resistance, hepatic steatosis and neurodegenerative diseases (Mayr, 2015).

Mitochondrial morphology is continuously reshaped by opposing fusion and fission dynamics (Putti et al., 2015). Fusion promotes organelle elongation and network connectivity, enabling the exchange of mitochondrial deoxyribonucleic acid (DNA) and matrix components, thereby sustaining mitochondrial integrity and bioenergetic efficiency (Westermann, 2010). Fusion activity is often enhanced under conditions of

metabolic stress or elevated energy demand, such as during fasting or CR, to support oxidative phosphorylation (Mishra & Chan, 2016).

Fission, in contrast, enables the segregation and removal of damaged mitochondria segments and supports adaptation to bioenergetic stress (Mishra & Chan, 2016; Westermann, 2010). While fission is an essential component of mitochondrial quality control, excessive or unbalanced fission, without adequate compensatory fusion, disrupt mitochondrial homeostasis and impairs cellular function (Chen et al., 2005; Putti et al., 2015).

Mitochondrial dynamics are tightly coupled to lipid metabolic pathways. Alterations in dietary fat composition and energy availability can therefore differentially affect mitochondrial function through coordinated changes in both lipid metabolism and mitochondrial architecture (Frohman, 2015).

1.3 Role of Heart and Liver Metabolism

The liver and heart are metabolically active organs with central roles in maintaining systemic energy homeostasis (Da Dalt et al., 2023; P. Nguyen et al., 2008). Their function critically depends on mitochondrial activity and both adapt dynamically to changes in dietary composition, though in fundamentally different ways (Labarthe et al., 2008).

1.3.1 Heart

The heart never stops working and its continuous contractile activity requires an uninterrupted and efficient supply of energy (H. Wang et al., 2023). Under resting and fasting conditions, mitochondrial β-oxidation of LCFAs provides roughly 60-70 % of cardiac adenosine triphosphate (ATP) production, with the remaining fraction derived from glucose, lactate, pyruvate and ketone bodies (Dikalov et al., 2024; Longnus et al., 2001). Although the heart can adjust substrate utilization in response to availability, it remains critically dependent on intact mitochondrial function and sustained FAO capacity (Pascual & Coleman, 2016).

Disruptions in cardiac lipid metabolism or an imbalance between mitochondrial fusion and fission can lead to lipid accumulation, oxidative stress and impaired contractility, thereby contributing to cardiovascular dysfunction (B. Y. Nguyen et al., 2019). Accordingly, dietary interventions, including intermittent fasting (IF) or MCT-enriched diets, have been proposed to modulate cardiac substrate utilization and mitochondrial efficiency (Hailu et al., 2024; Labarthe et al., 2008). Early studies using perfused rat

hearts demonstrated that replacing LCFAs with MCFAs increased acetyl-CoA availability and β-oxidation rates while reducing glucose utilization, suggesting a potential metabolic advantage of MCTs for cardiac function (Labarthe et al., 2008).

However, more recent evidence indicates that the capacity for carnitine-independent MCFA oxidation is tissue-specific and largely restricted to the liver and kidney. In contrast, the heart and skeletal muscle appear unable to oxidize fatty acids from any chain length (C6-C18) without carnitine. This suggests that MCFAs do not bypass CPT1 regulation in cardiac tissue (Pereyra et al., 2023). This discrepancy is important when interpreting how MCT-enriched diets effect cardiac metabolism.

Beyond substrate utilization, mitochondrial structure is essential for sustaining cardiac function (B. Y. Nguyen et al., 2019). Heart failure, both in humans and in experimental is associated with mitochondrial fragmentation, with reduced expression of fusion-related genes such as mitofusin 1 and 2 (*MFN1/2*) and optic atrophy 1 (*OPA1*), alongside increased expression of fission-related genes including mitochondrial fission 1 protein (*FIS1*) (T. He et al., 2025; Javadov et al., 2011; B. Y. Nguyen et al., 2019). This imbalance promotes oxidative stress, impairs ATP production and disrupts calcium homeostasis. Consistent with this, cardiac-specific deletion of both *MFN1* and *MFN2* in mice results in mitochondrial fragmentation and eccentric cardiac hypertrophy (Song et al., 2015, 2017). A tightly regulated balance of mitochondrial fusion and fission is therefore essential for preserving cardiac metabolic capacity and contractile function (B. Y. Nguyen et al., 2019).

1.3.2 Liver

The liver serves as the central organ for nutrient processing and energy regulation, showing a remarkable metabolic flexibility in response to nutrient availability (Rui, 2014). In the postprandial state, hepatic metabolism favors anabolic pathways, including de novo lipogenesis (DNL) and triglyceride synthesis, followed by lipid export via lipoproteins. In contrast, during fasting or carbohydrate-restriction, the liver shifts toward catabolic pathways such as β-oxidation and ketogenesis.

Under these conditions, enhanced FAO generates acetyl-CoA at a rate that exceeds the capacity of the TCA cycle. The resulting accumulation is redirected toward ketone body production, predominantly acetoacetate and β-OHB, which are released into the circulation and serve as alternative energy substrates for peripheral tissues, including the heart. This supports systemic energy homeostasis (Huang et al., 2020).

This metabolic flexibility is coordinated by nutrient-sensitive transcription factors. In states of carbohydrate-rich conditions, insulin- and glucose-dependent activation of transcription factors such as sterol regulatory element-binding protein 1c (SREBP-1c) promotes the expression of lipogenic genes like acetyl-CoA carboxylase alpha (*ACACA*) and fatty acid synthase (*FASN*) (Rui, 2014; Tian et al., 2016). During energy-restricted conditions, the liver shifts toward fat oxidation. Peroxisome proliferator-activated receptor alpha (PPARα) induces the expression of genes involved in FAO and ketone metabolism, such as acyl-CoA dehydrogenase medium chain (*ACADM***)** and carnitine acetyltransferase (*CRAT***)**, thereby increasing mitochondrial oxidative capacity (Rui, 2014).

This transcriptional switch between anabolic and catabolic states is coordinated by energy-sensing kinases that act upstream of both SREBP-1c and PPARα. Under fasting conditions or carbohydrate restriction, falling insulin levels and a rising adenosine monophosphate (AMP)/ATP ratio activate AMP-activated protein kinase (AMPK), which in turn inhibits mTOR complex 1 (mTORC1) signaling. This suppresses SREBP-1c-driven lipogenesis and simultaneously promotes PPARα-dependent transcription of FAO genes (Rui, 2014; Kersten, 2014; Marcondes-de-Castro et al., 2023). Conversely, in the postprandial state, mTORC1 activation leads to anabolic pathways by supporting SREBP-1c processing and suppressing PPARα activity (Marcondes-de-Castro et al., 2023). This AMPK-mTORC1- PPARα axis therefore represents a central node through which dietary fat composition translates into tissue-specific gene expression changes, including those targeted in the present study.

Given its high mitochondrial content and oxidative capacity, the liver plays a key role in coordinating substrate availability for peripheral organs. Dietary interventions that promote a catabolic metabolic state, including KDs and CR, have been associated with reduced hepatic lipid accumulation, improved insulin sensitivity and enhanced mitochondrial FAO (Emanuele et al., 2025). These adaptations reflect a coordinated metabolic shift toward lipid utilization and ketone body production that supports energy-demanding tissues such as the heart (Milder & Patel, 2012; Rui, 2014; Schönfeld & Wojtczak, 2016). The transcriptional and enzymatic mechanisms underlying this shift are further addressed in the following chapter.

1.4 Ketogenic Diets and Their Protective Effects

KDs, characterized by very low carbohydrate, moderate protein and high fat intake, induce a metabolic shift toward FAO and hepatic ketogenesis (Longo et al., 2019; Roslund et al., 2025). Under these conditions, enhanced mitochondrial β-oxidation in hepatocytes generates acetyl-CoA beyond TCA cycle capacity, which is consequently redirected toward ketone body synthesis. As shown in Figure 1, this process involves the sequential action of 3-hydroxy-3-methylglutaryl-CoA synthase 2 (HMGCS2), 3-hydroxy-3-methylglutaryl-CoA lyase (HMGCL) and 3-hydroxybutyrate dehydrogenase 1 (BDH1), producing β-OHB, acetoacetate and acetone (Mooli & Ramakrishnan, 2022). These ketone bodies are exported via monocarboxylate transporters and taken up as alternative energy substrates by extrahepatic tissues, such as the heart (Emanuele et al., 2025).

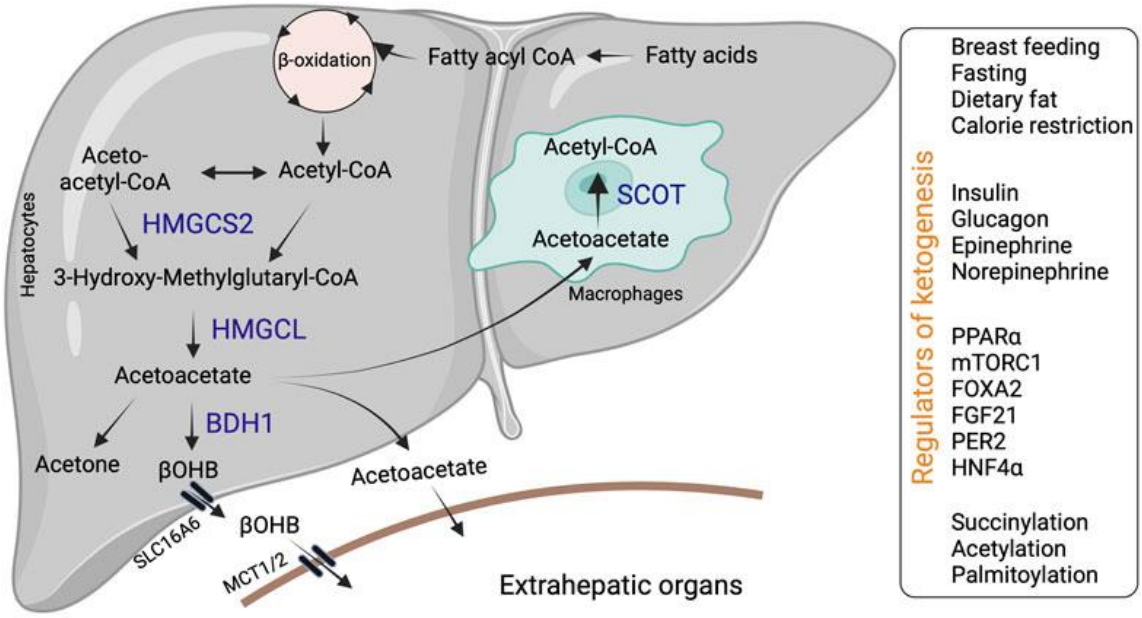

Figure 1: Hepatic ketogenesis and its regulators. *Under conditions of low carbohydrate availability hepatic fatty acid β-oxidation generates acetyl-CoA, which exceeds the capacity of the tricarboxylic acid cycle and is redirected toward ketogenesis. In hepatocytes, acetyl-CoA is converted to acetoacetyl-CoA and subsequently to acetoacetate via the key ketogenic enzymes HMGCS2 and HMGCL. Acetoacetate can be reduced to β-OHB or spontaneously converted to acetone. Ketone bodies are exported from the liver via monocarboxylate transporters (e.g. MCT1/2, SLC16A6) and taken up by extrahepatic tissues. In peripheral organs, acetoacetate is reconverted to acetyl-CoA by SCOT and enters mitochondrial oxidative metabolism. Ketogenesis is tightly regulated by hormonal signals (e.g. low insulin and high glucagon), transcriptional regulators such as PPARα or mTORC1, as well as post-translational modification.; BDH1 3-Hydroxybutyrate dehydrogenase 1, HMGCL 3-hydroxy-3-methylglutaryl-CoA lyase; HMGCS2 3-Hydroxy-3-methylglutaryl-CoA synthase; MCT1/2 Monocarboxylate transporter 1/2; mTORC1 Mechanistic target of rapamycin complex 1; PPARα Peroxisome proliferator-activated receptor alpha; SCOT Succinyl-CoA:3-ketoacid CoA-transferase; SLC16A6 Solute carrier family 16 member 6; β-OHB β-Hydroxybutyrate (Mooli & Ramakrishnan, 2022)*

The resulting metabolic state resembles prolonged fasting, characterized by reduced insulin and glucose levels, depletion of hepatic glycogen stores and enhanced mitochondrial lipid oxidation (Longo et al., 2019). Reduced insulin signaling suppresses lipogenic enzymes such as acetyl-CoA carboxylase 1 (ACC1) and 2 (ACC2), encoded by *ACACA* and acetyl-CoA carboxylase beta (*ACACB*). This leads to decreased malonyl-CoA levels and relief of CPT1 inhibition, facilitating mitochondrial fatty acid entry and oxidation (Cao et al., 2023; Dong et al., 2024). PPARα simultaneously promotes expression of genes such as *ACADM* and *CRAT*, supporting mitochondrial β-oxidation and acetyl-CoA buffering (Rui, 2014).

Beyond substrate metabolism, KDs also show beneficial effects on mitochondrial structure and function. Reduced insulin signaling suppresses DNL and hepatic lipid accumulation, contributing to improved insulin sensitivity (Paoli et al., 2023). Ketogenic conditions have additionally been associated with enhanced mitochondrial biogenesis and improved respiratory capacity (Milder & Patel, 2012; Tang et al., 2025). Notably, the liver produces ketone bodies but cannot use them due to the lack of succinyl-CoA:3-oxoacid-CoA transferase (SCOT), thereby ensuring that hepatically produced ketones are efficiently exported to peripheral tissues (Kolb et al., 2021; Mooli & Ramakrishnan, 2022)

Importantly, the metabolic effects of KDs are further shaped by dietary fat composition. MCT-enriched KDs have been shown to increase mitochondrial respiratory capacity and reduce inflammatory signaling (Hecker et al., 2014; S. Yu et al., 2019). Compared to LCTs, MCTs undergo more rapid hepatic oxidation, resulting in a more pronounced and rapid increase in ketone levels (Sternberg et al., 2023). In addition to their role as energy substrates, ketone bodies, particularly β-OHB, function as signaling molecules that attenuate oxidative stress and inflammation, thereby contributing to tissue protection under metabolic stress (Dunn et al., 2023). While these effects were initially described in the brain, this ketone-mediated signaling role is increasingly recognized across multiple tissues, including the liver and heart (Anekwe et al., 2020; Peng et al., 2018; Sternberg et al., 2023).

Collectively, the reduction of glucose and insulin signaling under KD conditions promotes a shift away from lipogenesis toward mitochondrial FAO in metabolic active tissues (D C. Harvey et al., 2018; Sternberg et al., 2023). This dynamic of hepatic ketone production and extrahepatic ketone utilization underscores the potential of KDs,

particularly when enriched with MCTs, to improve metabolic health through modulation of mitochondrial lipid metabolism.

1.4.1 Regulation of De Novo Fatty Acid Synthesis: Acetyl-CoA Carboxylase Alpha

ACCs are central regulatory enzymes in lipid metabolism that catalyze the ATP-dependent carboxylation of acetyl-CoA to malonyl-CoA (Figure 2). Malonyl-CoA has a dual function both as the committed substrate for DNL and as an inhibitor of mitochondrial β-oxidation through suppression of CPT1 (Harada et al., 2007; Longo et al., 2019).

In mammals, two ACC isoforms exist: ACC1, encoded by *ACACA,* and ACC2, encoded by *ACACB* (K.-H. Kim, 1997). ACC1 is predominantly expressed in lipogenic tissues such as the liver and white adipose tissue and is localized in the cytosol (Harada et al., 2007; X. Li & Bi, 2023; Tamura et al., 2021). Its activity is upregulated in response to high-carbohydrate diets and elevated insulin levels. Under these conditions, insulin signaling induces dephosphorylation and activation of ACC1 via insulin-sensitive protein phosphatases, thereby promoting DNL. The resulting increase in cytosolic malonyl-CoA provides substrate for fatty acid synthase, predominantly promoting the synthesis of LCFAs (Tamura et al., 2021; Y. Wang et al., 2022).

ACC1 activity is also controlled by cellular energy status. Activation of AMPK under conditions of energy deprivation leads to phosphorylation and inhibition of ACC1, reducing malonyl-CoA production. This mechanism suppresses DNL while indirectly favoring FAO (Galic et al., 2018). Under ketogenic conditions, ACC1 is further regulated at the post-translational level. KDs reduce malonylation of ACC1, leading to decreased enzyme activity and protein stability, which contributes to suppression of DNL and protection against hepatic steatosis (Cao et al., 2023).

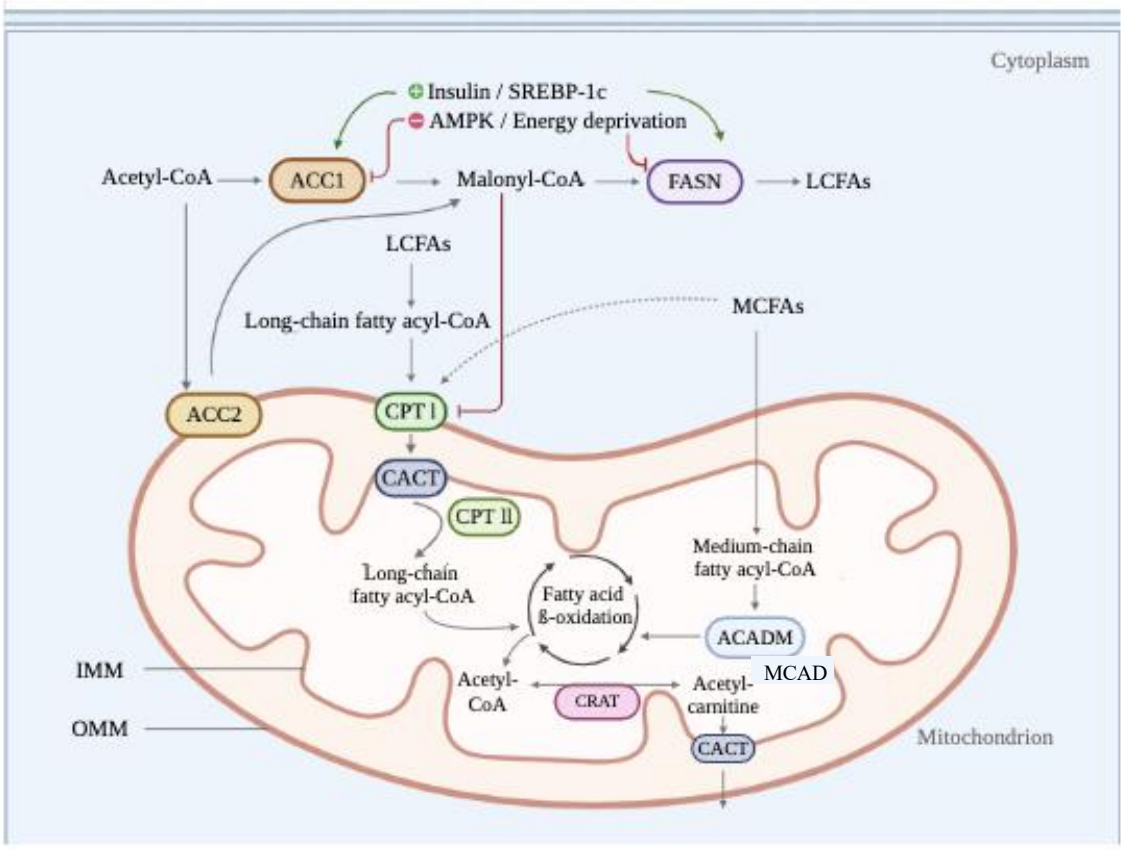

Figure 2: Schematic overview of key pathways involved in de novo lipogenesis, fatty acid transport and mitochondrial β-oxidation. *Acetyl-CoA carboxylases 1 (ACC1) and fatty acid synthase (FASN) regulate cytosolic fatty acid synthesis, whereas acetyl-CoA carboxylases 2 (ACC2)-derived malonyl-CoA modulates mitochondrial fatty acid uptake via carnitine palmitoyl-transferase (CPT1). Long-chain fatty acids (LCFAs) require transport through the carnitine shuttle (CPT1, Carnitine-acylcarnitine translocase (CACT), CPT2) prior to β-oxidation, while medium-chain fatty acids (MCFAs) can predominantly enter mitochondria independently of CPT1. Medium-chain acyl-CoA dehydrogenase (MCAD) and carnitine acetyltransferase (CRAT) are involved in MCFAs oxidation and acetyl-CoA buffering, respectively. AMPK AMP-activated protein kinase; IMM Inner mitochondrial membrane; OMM Outer mitochondrial membrane; SREBP-1c Sterol regulatory element-binding protein 1c [Created by author using BioRender.com].*

Although malonyl-CoA produced by ACC1 can indirectly influence mitochondrial FAO via CPT1 inhibition, this regulatory function is more directly controlled by the mitochondrial isoform ACC2, as described in the following section (Harada et al., 2007).

Given its central role in cytosolic lipid flux, alterations in *ACACA* expression and ACC1 activity represent a key regulatory node between dietary interventions and mitochondrial energy metabolism in both liver and heart.

1.4.2 Regulation of Mitochondrial Fatty Acid Entry: Acetyl-CoA Carboxylase Beta

In contrast to ACC1, which primarily supports cytosolic DNL, ACC2 is predominantly expressed in oxidative tissues such as heart and skeletal muscle and is localized to the

outer mitochondrial membrane (OMM) (X. Li & Bi, 2023; Y. Wang et al., 2022). From this position, it directly controls mitochondrial fatty acid entry rather than cytosolic lipid synthesis.

ACC2 catalyzes the conversion of acetyl-CoA to malonyl-CoA at the mitochondrial surface. The locally produced malonyl-CoA acts as an inhibitor of CPT1, which limits the mitochondrial uptake of long-chain fatty acyl-CoAs into the matrix and their subsequent β-oxidation (Harada et al., 2007).

Under nutrient-rich conditions, particularly following high-carbohydrate intake, insulin promotes the dephosphorylation and activation of ACC2. This leads to elevated mitochondrial malonyl-CoA concentrations and inhibition of CPT1, which suppresses LCFA β-oxidation and shifts metabolism towards lipid storage (Dong et al., 2024; Witters & Bacon, 1985). Conversely, during fasting, reduced blood glucose levels and a rising AMP/ATP ratio activate AMPK. This subsequently phosphorylates and inhibits ACC2, reducing malonyl-CoA levels at the OMM (Galic et al., 2018; Longo et al., 2019). This reduced malonyl-CoA concentration lifts the inhibition of CPT1, resulting in increased mitochondrial fatty acid uptake and enhanced β-oxidation (Dong et al., 2024; Galic et al., 2018; Longo et al., 2019).

The functional impact of ACC2-derived malonyl-CoA depends critically on which CPT1 isoform is present. The liver expresses CPT1A, which has relatively moderate malonyl-CoA sensitivity, while the heart muscle, which predominantly expresses CPT1B, is approximately 100-fold more sensitive to malonyl-CoA inhibition (Schreurs et al., 2010).

Taken together, ACC2 controls the balance between lipid oxidation and storage by regulating mitochondrial fatty acid entry. Diet-induced or fasting-related changes in *ACACB* expression will translate into functionally distinct outcomes depending on the tissue.

1.4.3 Terminal Step of De Novo Lipogenesis: Fatty Acid Synthase

Fatty acid synthase (FASN), encoded by *FASN*, is a cytosolic enzyme complex predominantly expressed in lipogenic tissues such as the liver, white adipose tissue and lactating mammary gland (Meade et al., 2025; Shi et al., 2019) A mitochondrial form of FASN exists (Wedan et al., 2024) but is not the focus of this study.

FASN catalyzes the terminal step of DNL by condensing acetyl-CoA and malonyl-CoA into palmitate (C16:0), using nicotinamide adenine dinucleotide phosphate (NADPH) as

a reductant (Jensen-Urstad & Semenkovich, 2012; Meade et al., 2025). This process is closely linked to ACC1 activity, which provides the precursor malonyl-CoA (Figure 2) (Ruiz-Pérez et al., 2021; Wu et al., 2014).

FASN expression is sensitive to nutritional status. Under carbohydrate-rich and insulin-stimulated conditions, *FASN* is upregulated through lipogenic transcription factors such as SREBP-1c, supporting fatty acid synthesis for membrane production and energy storage (Berndt et al., 2007; Terry & Hay, 2024). Diets rich in PUFAs suppress *FASN* expression through negative feedback mechanisms, limiting endogenous lipogenesis when exogenous fatty acids are abundant (Moon et al., 2002). KDs have similarly been shown to markedly downregulate hepatic *FASN* expression (Kennedy et al., 2007; Nasser et al., 2022). During energy-restricted states, reduced insulin levels and increased AMPK activity further suppress lipogenic pathways, thereby reducing *FASN* expression and shifting metabolism from DNL toward mitochondrial FAO (Trepiana et al., 2018).

1.4.4 Mitochondrial β-Oxidation and Acetyl-CoA Buffering: Acyl-CoA Dehydrogenase Medium Chain and Carnitine Acetyltransferase

The *ACADM* gene encodes medium-chain acyl-CoA dehydrogenase (MCAD), a mitochondrial flavoenzyme catalyzing the first step of medium-chain FAO (Madeira et al., 2023). MCAD acts on acyl-CoA esters with chain lengths from C4 to C14, with highest catalytic efficiency toward C6-C12 substrates and maximum activity toward octanoyl-CoA (C8) (Lim et al., 2018; Satoh, 2003). By initiating the dehydrogenation of medium-chain fatty acyl-CoAs to trans-2-enoyl-CoA, MCAD enables subsequent β-oxidation steps and efficient ATP production (J. J. Kim et al., 1993; Y. Wang et al., 2010). Functionally, *ACADM* acts in direct contrast to the anabolic pathway of lipid synthesis, regulated by *ACACA*, *ACACB* and *FASN*.

ACADM is highly expressed in the liver and heart, consistent with their dependence on FAO for energy production. In the liver, *ACADM* is further upregulated under conditions of fasting or carbohydrate restriction, when FAO becomes the central catabolic pathway (Matyi et al., 2018; Nagao et al., 1993; Zhang et al., 1997). These transcriptional adaptations are mediated in part by PPARα (Gulick et al., 1994). Collectively, this regulation makes *ACADM* expression a useful marker of the liver's oxidative state.

Once MCAD initiates β-oxidation, the resulting acetyl-CoA requires metabolic control to prevent accumulation. CRAT is a mitochondrial enzyme that reversibly catalyzes the transfer of acetyl groups between acetyl-CoA and carnitine, generating acetylcarnitine

and free CoA (Volpicella et al., 2025). This reaction buffers intracellular acetyl-CoA concentrations and maintains an adequate pool of free CoA, which is particularly important in tissues with high oxidative demand (Dambrova et al., 2022). This study focuses on the CRAT isoform containing an N-terminal mitochondrial targeting sequence.

Beyond its buffering role, CRAT also indirectly regulates the pyruvate dehydrogenase complex (PDH), which controls the entry of glycolytic carbon into the TCA cycle (Altamimi et al., 2018; Dambrova et al., 2022). Elevated acetyl-CoA levels inhibit PDH activity, thereby slowing glucose oxidation. By converting acetyl-CoA to acetylcarnitine, CRAT relieves this inhibition and supports metabolic flexibility between lipid and carbohydrate oxidation (Koltai et al., 2021).

1.4.5 Outer Mitochondrial Membrane Fusion: Mitofusin 1 and Mitofusin 2

Mitochondria are highly dynamic organelles that continuously undergo fusion and fission to adapt to cellular energy demands, maintain structural integrity and preserve metabolic flexibility (Chandhok et al., 2018; Kyriazis et al., 2022). Mitochondrial fusion is particularly important for the exchanges of mitochondrial DNA and matrix contents, buffering against mutational damage and supporting efficient oxidative metabolism. The first step of OMM fusion is mediated by MFN1 and MFN2. Subsequent inner membrane fusion is carried out by OPA1 (Qi et al., 2016), addressed in the following section. An overview of mitochondrial fusion and fission processes is shown in Figure 3.

Both MFN1 and MFN2 are large transmembrane guanosine triphosphatases (GTPases) anchored in the OMM (Chandhok et al., 2018). They are expressed at comparable levels in the liver and at particularly high levels in the heart (Santel et al., 2003). Despite sharing roughly 80 % sequence homology they are not functionally redundant (Dai & Jiang, 2019). MFN1 has stronger GTPase activity and is essential for efficient membrane tethering and fusion, while MFN2 is further involved in processes beyond fusion, such as mitochondria endoplasmic reticulum (ER) tethering, calcium transfer and lipid exchange, mitophagy and apoptosis (Mann et al., 2024; Zaman & Shutt, 2022). Loss of either protein alone results in mitochondrial fragmentation. However, only the simultaneous deletion of both genes completely abolishes mitochondrial fusion (Dai & Jiang, 2019).

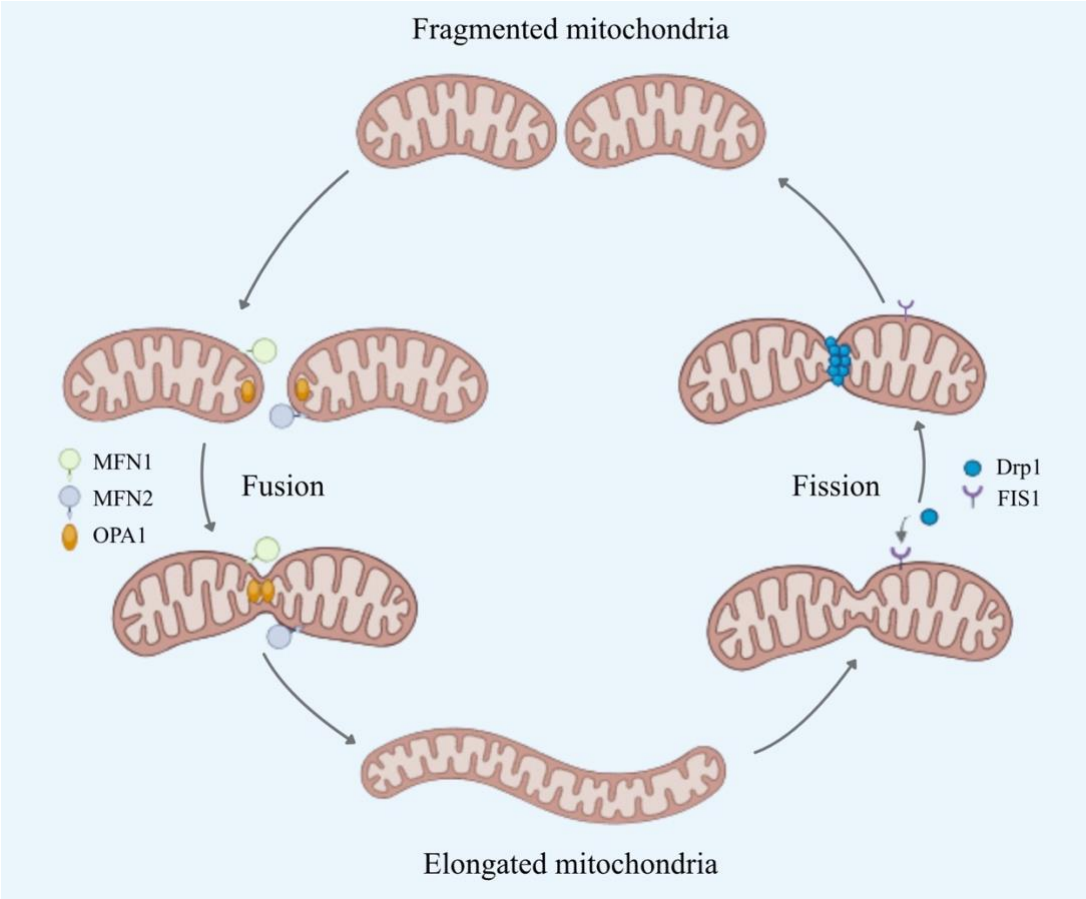

Figure 3: Schematic representation of mitochondrial fusion and fission. *MFN1 and MFN2 mediate outer mitochondrial membrane (OMM) fusion, while OPA1 regulates inner membrane fusion, resulting in elongated mitochondria. Conversely, FIS1-dependent recruitment of Drp1 to the OMM induces mitochondrial fission and fragmentation. Drp1 Dynamin-related protein 1; FIS1 Mitochondrial fission protein 1; MFN1 Mitofusin 1; MFN2 Mitofusin 2; OPA1 Optic atrophy protein 1 [Created by author using BioRender.com and Canva.com, adapted from Lee et al. (2024)].*

Both MFN1 and MFN2 are sensitive to nutritional status. CR has been shown to upregulate mitofusin expression, suggesting that enhanced fusion protects mitochondrial integrity under energy-limited conditions (Rodríguez-López et al., 2020). Similarly, KDs have been reported to increase *MFN2* in hepatic tissue (Newell et al., 2016).

In the heart, intact mitochondrial fusion dynamics contribute to metabolic stability and protection against oxidative stress (Da Dalt et al., 2023) Since both the heart and liver are metabolically active organs with high energetic demand, modulations in *MFN1/2* expression may reflect adaptive or maladaptive mitochondrial responses to altered nutrition.

1.4.6 Inner Mitochondrial Membrane Fusion: Optic Atrophy 1

OPA1 encodes a dynamin-like GTPase at the inner mitochondrial membrane (IMM), where it mediates inner membrane fusion, shapes cristae morphology and protects

mitochondrial genome integrity (Rahn et al., 2013; Von Der Malsburg et al., 2023; Zhang et al., 2011). Through alternative splicing and proteolytic processing, multiple OPA1 isoforms are generated, enabling fine-tuned regulation of these functions (L. Li et al., 2019; Rahn et al., 2013).

OPA1-mediated fusion of the IMM is essential for maintaining intact cristae structure, which in turn is critical for efficient respiratory chain assembly and oxidative phosphorylation (Zhang et al., 2011). Disruption of OPA1 destabilizes cristae, leading to reduced respiratory efficiency, loss of membrane potential and increased vulnerability to apoptosis (Burke et al., 2015).

These effects are particularly pronounced in high-energy-demanding tissues. In cardiomyocytes, even partial OPA1 deficiency leads to impaired mitochondrial respiration, reduced mitochondrial DNA copy number and the development of late-onset cardiomyopathy (Burke et al., 2015). In the liver, the role of OPA1 appears more context dependent. While OPA1 is essential for mitochondrial integrity and cell survival under normal conditions, experimental depletion has been shown to attenuate steatosis in non-alcoholic fatty liver disease models, suggesting that compensatory mechanisms can partially offset the loss of OPA1 in a lipid-overload context (H. Lee et al., 2023). Studies using high-fat diet models have further documented a downregulation of *OPA1* expression across several metabolic tissues, including heart and liver (Zheng et al., 2023).

Overall, OPA1 therefore connects IMM dynamics, respiratory efficiency and metabolic adaptation, making it a relevant target in studies examining dietary effects on mitochondrial function.

1.4.7 Mitochondrial Fission: Fission Protein 1

While fusion promotes connectivity and metabolic efficiency, fission enables the segregation and removal of dysfunctional mitochondrial segments via mitophagy (Qi et al., 2016; R. Yu et al., 2019). An appropriate balance between fission and fusion is essential for mitochondrial quality control and cellular health (Tokuyama & Yanagi, 2023; R. Yu et al., 2019).

Mitochondrial fission is primarily executed by the cytosolic GTPase dynamin-related protein 1 (Drp1), which is recruited to the OMM by adaptor proteins. Among the known Drp1 receptors, including mitochondrial fission factor, mitochondrial dynamics protein 49 (MiD49) and MiD51, FIS1 has also been proposed to contribute to Drp1 recruitment,

although its precise contribution remains debated in the mammalian context (Gomes & Scorrano, 2008; Palmer et al., 2013). Upon OMM recruitment, Drp1 oligomerizes around the mitochondrial membrane, leading to membrane constriction and ultimately division of the organelle into two daughter mitochondria (Zerihun et al., 2023). FIS1 is a tail-anchored OMM protein whose cytosolic domain contains tetratricopeptide repeat motifs that mediate protein-protein interactions relevant to fission (Ihenacho et al., 2021; Y. Lee et al., 2004). Beyond Drp1 recruitment, FIS1 has been shown to inhibit mitochondrial fusion by interfering with OPA1 and mitofusin function (Ihenacho et al., 2021; R. Yu et al., 2019).

FIS1 overexpression induces mitochondrial fragmentation and apoptosis, whereas its knockdown promotes mitochondrial elongation (Y. Lee et al., 2004; Tokuyama & Yanagi, 2023). In cardiac tissue, defective fission dynamics have been associated with mitochondrial fragmentation, contractile dysfunction and cardiomyopathy (Tokuyama & Yanagi, 2023).

Beyond its involvement in fission, FIS1 participates in mitophagy and has been implicated in the regulation of inflammatory signaling and cellular stress responses (Liou et al., 2022). In the context of metabolic diseases, hepatic FIS1 upregulation has been shown to improve glucose homeostasis and reduce oxidative stress in high-fat diet-fed mice by promoting mitophagy, suggesting a protective role in dietary lipid stress situation (Liou et al., 2022).

1.4.8 Cellular Stress Response and Metabolic Adaptation: Tumor Protein p53

The *Trp53* gene encodes the murine p53 tumor suppressor, the ortholog of human *TP53*. Initially described as the “guardian of the genome” for its roles in cell cycle arrest, DNA repair, senescence and apoptosis (Han et al., 2022; Hernández Borrero & El-Deiry, 2021; National Center for Biotechnology Information, 2026), p53 is now recognized as a broader metabolic regulator with roles in mitochondrial function and energy adaptation (S. Yu et al., 2022).

In mice, the *Trp53* gene gives rise to two primary transcripts. Transcript variant 1 encodes the canonical, full-length protein Mp53α (*Trp53* (l)), the murine equivalent of the human p53α. Transcript variant 2 encodes the shorter isoform Mp53AS (*Trp53* (s)), which arises through alternative splicing of a 3’ splice site in intron 10, replacing the last 26 amino acids of the α C-terminus with 17 alternative residues (Joruiz & Bourdon, 2016; Marcel et al., 2011). Both isoforms retain the DNA-binding and oligomerization domains,

enabling them to form hetero-tetramers with one another. This co-oligomerization matters functionally: Whereas Mp53AS expressed alone promotes apoptosis in response to cellular stress, co-expression of Mp53AS attenuates this apoptotic response, thereby modulating the p53 stress program rather than executing it (Almog et al., 2000).

In hepatocytes, p53 is stabilized during fasting in an AMPK-dependent manner and contributes to adaptive regulation of FAO, amino acid catabolism and gluconeogenesis (Oster et al., 2022; Prokesch et al., 2017). Acute liver-specific deletion of p53 impairs these adaptive responses, promoting triglyceride accumulation and disturbed glycogen homeostasis (Katz et al., 2012; Oster et al., 2022). The precise role of p53 in hepatic steatosis remains context-dependent and partly conflicting across models, as the outcome is shaped by isoform composition and co-regulatory factors (S. Yu et al., 2022).

In the heart, p53 is essential for embryonic cardiac development and normal myocardial architecture. Under pathological stress, including myocardial infarction or cardiomyopathy, p53 expression is elevated. This promotes mitochondrial metabolic reprogramming and apoptosis, processes that can contribute to maladaptive cardiac remodeling (Men et al., 2021). Recent findings indicate that KDs activate cardiac p53 alongside upregulation of its downstream effector p21, indicating cellular stress and senescence signaling as a consequence of sustained ketogenic conditions (Wei et al., 2024).

In the context of this study, *Trp53* was included as a transcriptional indicator of cellular stress. Given the sensitivity of p53 to nutrient availability, changes in *Trp53* expression in hepatic and cardiac tissue may reflect the degree of metabolic stress induced by the different dietary interventions.

1.5 Aim of the Study

The study investigated how dietary fatty acid composition influences the transcriptional regulation of genes involved in lipid metabolism, mitochondrial dynamics and cellular stress responses in the liver and heart. Specifically, it compared the effects of a KD enriched in MCTs against a mixed LCT/MCT KD, two diets comparable in total fat content but markedly different fatty acid profiles, differing in the pathways of mitochondrial fatty acid uptake, oxidation and metabolic handling.

Given the distinct roles of liver and heart in energy homeostasis, gene expression changes were analyzed in both tissues to characterize organ-specific transcriptional adaptations to altered dietary fat composition. Target genes were selected to cover key regulatory pathways of DNL (*ACACA, ACACB, FASN)*, mitochondrial FAO (*ACADM, CRAT*), mitochondrial fusion (*MFN1, MFN2, OPA1*), fission (*FIS1*) and cellular stress signaling (*Trp53*).

To separate the effects of dietary fat composition from those of reduced calorie intake, CR and IF groups were included as reference conditions. This allowed discrimination between diet composition-specific transcriptional changes and those arising from reduced calorie intake per se.

Overall, this study aimed to provide insight whether distinct dietary lipid profiles, beyond their quantity, modulate mitochondrial gene expression in a tissue-specific manner.

2. Materials and Methods

2.1 Materials

This section describes the laboratory samples, experimental diets, chemicals and kits, and the primers used in this study.

2.1.1 Laboratory Samples and Diets

Male C57BL/6NRJ mice were used in this study. This well-established inbred strain is widely used in metabolic research (Smoczek et al., 2020) Tissue samples were provided by Sternberg et al. and have been described in detail previously (Gregor et al., 2022; Sternberg et al., 2023). The experimental diets were formulated and supplied by ssniff Spezialdiäten GmbH (Germany) and are summarized in Table 1. Detailed macronutrient compositions are provided in Table 4.

Table 1: Overview of the experimental diets

Diet	Product Number	Company
SD	S9139-E028	ssniff
CR	V153xR/M-H auto	ssniff
IF	V153xR/M-H auto	ssniff
LCT/MCT	S9139-E032	ssniff
LCT	S9139-E025	ssniff

CR Calorie restriction; IF Intermittent Fasting; LCT Long-chain triglyceride; MCT Medium-Chain triglyceride; SD Standard diet

2.1.2 Chemicals and Kits

Table 2 lists all kits and reagents used in this study in alphabetical order. Standard laboratory equipment, including plates, tubes and pipette tips were sourced from Roth (Austria), VWR (Austria) and Eppendorf (Austria).

Table 2: Alphabetically listed kits and reagents

Name	Product number	Company
Agarose	E476-500ML	Sigma-Aldrich
ChamQ Universal SYBR qPCR Master Mix	Q711-03	Vazyme
Chloroform	n.a.	Sigma-Aldrich
6x DNA Loading Dye	R0611	Thermo Fisher Scientific
4x gDNA Wiper Mix	R323-01-AB	Vazyme
Gene Ruler 100 bp DNA Ladder	SM0241	Thermo Fisher Scientific
Glycogen	R0561	Thermo Fisher Scientific
HiScript III qRT Supermix	R323-01-AC	Vazyme
Isopropanol	n.a.	Sigma-Aldrich
NF-H_2O	E476-500ML	VWR
5x No RT Control Mix	R323-01-AD	Vazyme
peqGreen DNA/RNA Dye	37-5000	peqlab
RNAse AWAY	7002	Molecular BioProducts
50x TAE-Electrophoresis Buffer	B49	Thermo Fisher Scientific

n.a. Not available

2.1.3 Primers

Table 3 summarizes all primers used for real-time quantitative polymerase chain reaction (RT-qPCR) analyses, including primer sequences, physicochemical properties and amplification characteristics. Listed parameters include primer name, direction (forward/ reverse), oligonucleotides sequences (5'→ 3'), primer length (base pairs; bp), guanine-cytosine content (GC, %), melting temperature (Tm, °C), amplicon size (bp) and experimentally determined amplification efficiency (%). Efficiency calculation is described in chapter 2.2.5.1. These parameters are essential to ensure specific, efficient and reproducible amplification.

Table 3: Primer sequences and key parameters for RT-qPCR

Primer Name	Direction	Sequence (5' → 3')	Primer length [bp]	GC [%]	TM [°C]	Amplicon length [bp]	Efficiency [%]	Company
mACACA	Forward	GCCGCCAGCCTGAGTTCTT	19	63.16	62.91	112	93.06	Microsynth
	Reverse	TGGCCAACGGAGATGGTTCA	20	55.00	61.77			Microsynth
mACACB	Forward	CTACAAGACGGGCGCAGGTCA	20	60.00	62.49	128	103.49	Microsynth
	Reverse	AGGCGCCAAACTTCAGCATC	20	55.00	61.59			Microsynth
mACADM	Forward	GGGGGAAAGGCCAACTGGTAT	21	57.14	62.10	151	101.18	Microsynth
	Reverse	AGCATCGCTGGCCCATGTTT	20	55.00	63.13			Microsynth
mCRAT	Forward	TGACTCGGCGACCTTGAACCTA	22	54.55	63.36	168	107.66	Microsynth
	Reverse	CCCAGGGGTTTTACCACGGTTC	22	59.09	63.36			Microsynth
mFASN	Forward	AACACGATCTGGTGCTGCCC	20	60.00	63.09	105	99.79	Microsynth
	Reverse	TGGGGGCTGTCGTGTCAGTA	20	60.00	63.01			Microsynth
mFIS1	Forward	GCTGGTTCTGTGTCCAAGAGCA	22	54.55	63.02	144	94.51	Microsynth
	Reverse	GACATAGTCCCGCTGTTCCTCT	22	54.55	61.53			Microsynth
mMFN1	Forward	CCAGGTACAGATGTCACCACAG	22	54.55	60.35	149	101.35	Microsynth
	Reverse	TTGGAGAGCCGCTCATTCACCT	22	54.55	63.98			Microsynth
mMFN2	Forward	TCCCTCTGACACCTGCCAAC	20	60.00	61.77	155	90.94	Microsynth
	Reverse	TGCCTTCCACACCACTCCTC	20	60.00	61.77			Microsynth
mOPA1	Forward	TCCACCACAGGAAGCTCAAGAAATC	25	48.00	63.01	141	102.34	Microsynth
	Reverse	TTTTCCCAGCACTCTGATCTCCAAC	25	48.00	63.01			Microsynth
mTrp53(s)	Forward	GCAGGGCTCACTCCAGCTAC	20	65.00	62.59	124	100.23	Microsynth
	Reverse	GTGATGGGGACGGGATGCAG	20	65.00	62.59			Microsynth
mTrp53(l)	Forward	TTCCGGGAGCTGAATGAGGC	20	60.00	62.26	93	96.30	Microsynth
	Reverse	TCTAGGCTGGAGGCTGGAGTG	21	61.90	63.04			Microsynth
mRPL4	Forward	GTATGGCACTTGGCGGAAGG	21	60.00	61.4	124	91.57	Microsynth
	Reverse	TGCTCGGAGGGCTCTTTGG	19	63.16	62.0			Microsynth
mTBP	Forward	CTACCGTGAATCTTGGCTGTAAAC	24	45.83	59.91	131	102.36	Microsynth
	Reverse	AATCAACGCAGTTGTCCGTGGC	22	54.55	64.42			Microsynth

ACACA Acetyl-CoA carboxylase alpha; ACACB Acetyl-CoA carboxylase beta; ACADM Medium-chain acyl-CoA dehydrogenase; bp Base pairs; CRAT Carnitine O-acetyltransferase; FASN Fatty acid synthase; FIS1 Mitochondrial fission protein 1; GC Guanine-Cytosine content; MFN1 Mitofusin 1; MFN2 Mitofusin 2; OPA1 Optic atrophy protein 1; Rpl4 Ribosomal protein L4; TBP TATA box binding protein; TM Melting temperature; Trp53 (l) Tumor protein p53, long isoform; Trp53 (s) Tumor protein p53, short isoform.

Target genes (*ACACA, ACACB, ACADM, CRAT, FASN, FIS1, MFN1, MFN2, OPA1* and *Trp53*) were selected based on their functional relevance to lipid metabolism and mitochondrial dynamics. TATA box binding protein (*TBP*) and ribosomal protein L4 (*RPL4*) were used as housekeeping genes (HKG) for normalization in both cardiac and hepatic tissue, as both have been validated as stably expressed reference genes under comparable experimental conditions (De Jonge et al., 2007; K. He et al., 2024). All primers, except for *RPL4*, which was kindly provided by Sternberg et al., were synthesized by Microsynth AG (Switzerland). Amplification efficiency was assessed by RT-qPCR and confirmed by agarose gel electrophoresis, as described in Chapter 2.2.4.

2.2 Methods

The following section describes the experimental workflow, including ribonucleic acid (RNA) isolation, complementary DNA (cDNA) synthesis, primer design and validation, and RT-qPCR.

2.2.1 Experimental Setup

Following birth, all mice were housed under controlled, specific-pathogen-free conditions at approximately 23 °C, with a 12-hour light/dark cycle. Animals were maintained in groups of three or five and provided with a standard chow diet for twelve weeks prior to dietary intervention. Based on the dietary model established by Sternberg et al. (2023), five dietary conditions were investigated: SD, CR, IF, LCT-enriched KD and LCT/MCT-enriched KD. The diets differed mainly in their carbohydrate and fat content (Table 4). Both KDs followed an 8:1 fat-to-carbohydrate ratio. SD, LCT and LCT/MCT diets were provided ad libitum.

The CR and IF groups received the same diet but under controlled feeding conditions. CR animals received 80 % of the standard daily caloric intake once per day. IF animals had ad libitum access to food for 24 hours, followed by a 24-hour fasting period. The day prior to euthanasia was designated as a fasting day. All animals had unrestricted access to water throughout the study.

Table 4: Nutrient composition of experimental diets

	SD	CR	IF	LCT/MCT	LCT
[MJ/kg]	15.1	12.9	12.9	29.7	29.7
Crude Protein [%]	16.1	19	19	8.1	8.1
Crude Fiber [%]	10.0	4.9	4.9	9.9	9.9
Crude Ash [%]	4.5	6.4	6.4	4.4	4.4
Crude Fat [%]	7.1	3.3	3.3	74.6	74.6
MCT [%]	0.1	n.s.	n.s.	25.76	1.1
LCT [%]	6.62	3.25	3.25	35.51	69.78
Unspecified fat sources [%]	0.38	0.05	0.05	13.33	3.72
Sugar [%]	6.0	4.7	4.7	1.0	1.0
Starch [%]	51.2	36.5	36.5	0	0
Other components	5.1	25.2	25.2	2.0	2.0

n.s. No Specification; CR Calorie restriction; IF Intermittent Fasting; LCT Long-chain triglyceride (diet); MCT Medium-chain triglyceride (diet); SD Standard Diet; % = weight/weight (w/w), i.e. g/100 g diet

All animals were maintained on their respective diets for a period of eight weeks. CR and IF groups received their respective interventions only during the last two weeks of the study period. All eight animals per group completed the study period under their respective dietary regimen without any loss. At 20 weeks of age, the mice were euthanized by inhalation of a Sevofluran overdose, followed by cardiac puncture for blood collection. Tissues from brain, heart, liver, skeletal muscle and brown adipose tissue were collected. The experimental timeline is illustrated in Figure 4.

All tissue samples analyzed in this study were obtained from animals used in previously conducted experiments (Gregor et al., 2022). No animal experiments were performed specifically for the present work, which is based exclusively on molecular biological analyses of pre-existing samples.

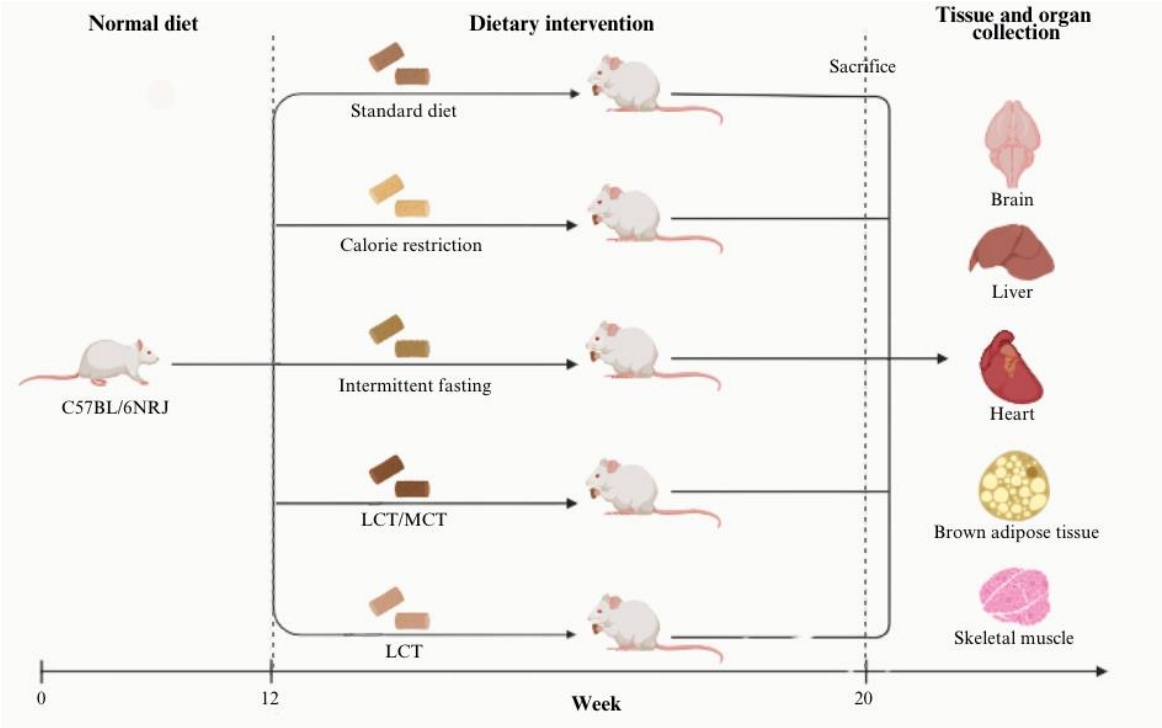

Figure 4: Schematic representation of the experimental design*. Male C57BL/6NRJ mice were initially maintained on a standard chow diet for 12 weeks before being randomly assigned to one of five dietary groups: Standard Diet (SD), Calorie Restriction (CR), Intermittent Fasting (IF), Long- and Medium-Chain Triglycerides ketogenic diet (LCT/MCT), or Long-Chain Triglycerides ketogenic diet (LCT). The SD, LCT, and LCT/MCT diets were administered for the full 8-week intervention period. CR and IF were introduced only in the final two weeks of the intervention, with animals receiving SD ad libitum before. At week 20, mice were euthanized, and brain, liver, heart, brown adipose tissue and skeletal muscle were collected for further analysis. Note: The schematic illustration depicts all five groups across the 8-week full intervention period for visual simplicity; CR and IF interventions were introduced only at week 18 [Created by author using BioRender.com].*

Tissue samples were immediately snap-frozen in liquid nitrogen to preserve RNA and protein integrity for downstream analyses. All animal experiments were conducted in collaboration with Kalina Duszka at the University of Vienna and approved by the Austrian national authority in accordance with §§ 26ff of the Animal Experiments Act (Tierversuchsgesetz 2012 – TVG 2012) under the permit number BMWFW-66.006/0008-V/3b/2018 (Sternberg et al., 2023).

2.2.2 Selection of Housekeeping Genes

RT-qPCR enables sensitive quantification of gene expression (Ren et al., 2021; Tatsumi et al., 2008). However, reliable results require normalization to reference genes, that are used to correct for technical variation across samples and must show stable expression across experimental conditions. Since no single gene is universally stable across all tissue types and experimental conditions, validation of appropriate HKGs for the specific experimental context is required (Ren et al., 2021).

In this study, *RPL4* and *TBP* were selected as reference genes. *RPL4* has been validated as a stable HKG in cardiac and hepatic tissue in metabolic studies (Brattelid et al., 2010; Tatsumi et al., 2008). *TBP* has similarly been shown to exhibit consistent expression levels in both tissues (Day et al., 2018; Ren et al., 2021; Tatsumi et al., 2008). The combined use of two independently validated HKG reduces the risk of systematic normalization bias.

2.2.3 RNA Isolation

RNA isolation was performed under stringent RNase-free conditions to preserve RNA integrity. Liver and heart tissues samples were stored at -80 °C until further processing. An overview of the RNA isolation workflow is shown in Figure 5.

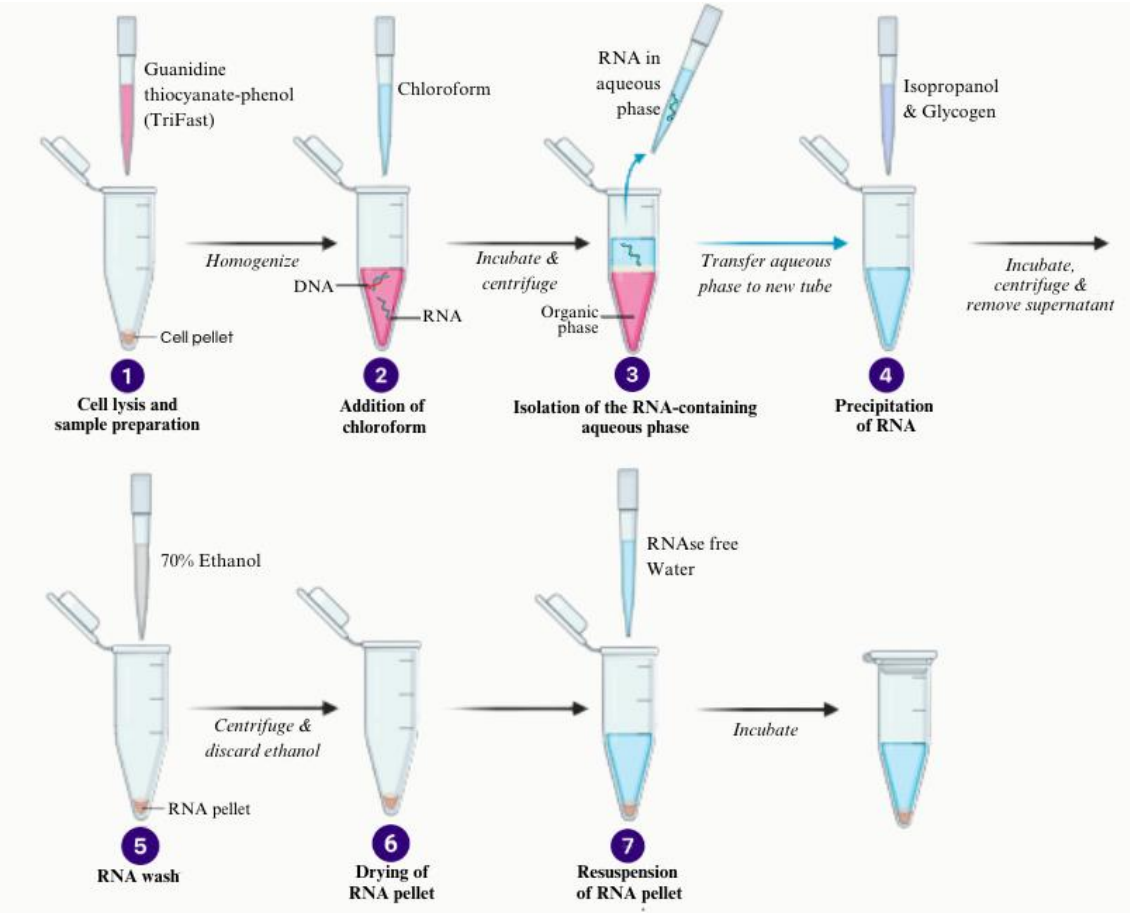

Figure 5: Schematic overview of the RNA isolation process. *Tissue samples were homogenized in TriFast, followed by phase separation using chloroform. RNA from the upper aqueous phase was precipitated with isopropanol and glycogen, washed with ethanol and dissolved in RNase-free water for downstream applications [Created by author using BioRender.com].*

2.2.3.1 Sample Preparation and Phase Separation

Frozen tissue samples were thawed on ice and homogenized in TriFast reagent (VWR). Phase separation was induced by the addition of 200 µL chloroform, followed by vortexing and incubation for 15 minutes at room temperature. Samples were centrifuged at 12.000 x *g* for 15 minutes at 4 °C, resulting in the formation of three distinct phases:

- An upper aqueous phase containing RNA,
- a middle interphase containing DNA, and
- a lower organic phase containing proteins and other contaminants (Figure 6).

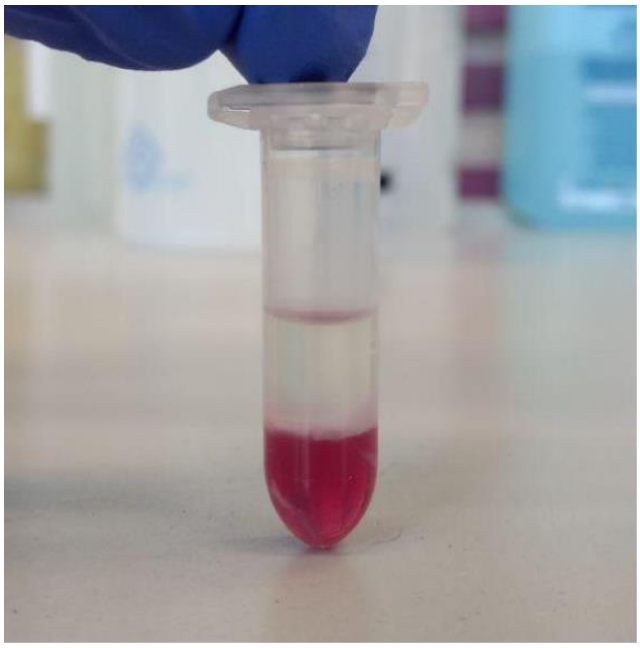

Figure 6: Phase separation during RNA isolation. *After homogenization and chloroform-induced phase separation, three phases were visible: The upper aqueous phase (RNA), middle interphase (DNA) and lower organic phase (proteins). This separation enables the selective extraction of RNA for downstream applications.*

The RNA-containing aqueous phase was carefully transferred to fresh RNAse-free tubes and placed on ice. The DNA-containing interphase was discarded. The organic phase was stored at 4 °C for potential downstream protein extraction.

2.2.3.2 RNA Precipitation and Resuspension

RNA was precipitated by adding 500 µL isopropanol and 2 µL glycogen to the aqueous phase. Glycogen was included to facilitate visualization of the RNA pellet. After gentle inversion and incubation for 10 minutes at room temperature, samples were centrifuged at 12.000 x *g* for eight minutes at 4 °C. The supernatant was discarded and the RNA pellet was washed twice with 1 mL of 70 % ethanol to remove residual contaminants.

Each wash step was followed by centrifugation at 7.500 x *g* for five minutes at 4 °C. The pellet was air-dried and dissolved in 50 µL RNase-free water. To ensure complete dissolution, samples were incubated at 60 °C for 10 minutes.

2.2.3.3 RNA Integrity and Purity Assessment

RNA concentration and purity were assessed spectrophotometrically using a NanoDrop system (Thermo Fisher Scientific). Absorbance at 260 nm was used to quantify RNA concentration, while the 260/280 nm ratio served as an indicator of protein contamination. Ratios close to 2.0 indicated sufficient purity and confirmed the suitability of the RNA samples for downstream applications.

2.2.4 cDNA Synthesis

To enable gene expression analysis via RT-qPCR, cDNA was synthesized from isolated RNA. All steps were performed under RNase-free conditions to prevent RNA degradation.

2.2.4.1 Removal of Genomic DNA

Prior to reverse transcription, residual genomic DNA (gDNA) was eliminated. RNA concentration was measured by Nanodrop. Sample volumes were adjusted to obtain up to
1 µg total RNA per reaction. For each sample, the following components were combined in RNase-free microcentrifuge tube:

- Template RNA (adjusted to required concentration),
- 4 µL 4x gDNA Wiper Mix,
- RNase-free ddH_2O to a final volume of 16 µL.

The mixture was gently pipetted up and down several times to ensure thorough mixing and was subsequently incubated at 42 °C for three minutes using a Rotor-Gene thermal cycler (Corbett Research).

2.2.4.2 Reverse Transcription Reaction

Following gDNA removal, reverse transcription was initiated by adding 4 µL 5x HiScript III qRT SuperMix (Vazyme) to each 16 µL reaction, resulting in a final volume of 20 µL. Samples were mixed gently to ensure homogeneity.

To control for potential gDNA contamination, a no-reverse-transcriptase (No RT) control was prepared in parallel. This consisted of a separate 16 µL gDNA-depleted RNA sample combined with 4 µL 5x No RT Control Mix (Vazyme).

2.2.4.3 Thermal Cycling Protocol

Reverse transcription was performed using the Rotor-Gene thermal cycler according to the temperature protocol in Table 5.

Table 5: Temperature protocol for cDNA synthesis

Temperature [°C]	25	37	50	85
Time [min]	10	10	10	6

After completion of the reaction, cDNA samples were diluted 1:5 with nuclease-free water (NF-H_2O) and stored at -20 °C for future use.

2.2.5 Primer Design and Validation

Primers for all target genes, except for *FIS1* and *MFN1*, were designed using the Primer-BLAST tool provided by the National Center for Biotechnology (NCBI) (National Center for Biotechnology Information, 2025). Coding DNA sequences were retrieved from the NCBI Nucleotide database and used as the template for in silico primer design. To ensure high amplification efficiency, the amplicon size was limited to a maximum of 200 bp.

Melting temperature parameters were set to a minimum of 60 °C, an optimal of 63 °C and a maximum of 66 °C to minimize the risk of non-specific amplification. Where possible, primers were designed to span exon-exon junctions to prevent amplification of residual gDNA. The target organism was specified as *Mus musculus* (TaxID: 10090). All remaining parameters were kept at default settings. Primer sequences for *FIS1* and *MFN1* were adopted from previously published sources (Origene Technologies, 2025a, 2025b).

All primers were synthesized and ordered from Microsynth AG (Switzerland). Upon delivery, each freeze-dried primer was resuspended in NF-H_2O to obtain stock solutions at a concentration of 100 µM. Working solutions were prepared by mixing 10 µL of each forward and reverse primer with 980 µL of NF-H_2O, resulting in a final concentration of 1 pmol/µL per primer. Primer specificity and amplification efficiency were subsequently validated by RT-qPCR, melting curve analysis and agarose gel electrophoresis.

2.2.5.1 Primer Efficiency Determination by RT-qPCR

Amplification efficiency was assessed using a serial dilution series. cDNA from liver and brown adipose tissue of CR mice was diluted 1:10 to generate a working solution, then serially diluted 1:3 to cover a broad concentration range.

RT-qPCR was performed in a total volume of 10 µL per well using a 384-well plate format. Each reaction was set up using a PCR master mix consisting of 5 µL ChamQ SYBR Master Mix (Vazyme), 1 µL NF-H_2O and 1 µL of the diluted cDNA. A total of 3 µL of the primer mix (containing forward and reverse primers) was additionally pipetted into each well. The plates were briefly centrifuged at 400 rpm for 10 seconds to ensure homogeneity before analysis on a Quant Studio™ 6 Flex RT-PCR System (Thermo Fisher Scientific).

Efficiency was determined by generating standard curves from the serial dilution series. Cycle threshold (Ct) values were plotted against the logarithm of the cDNA concentration. Linear regression analysis was used to calculate the slope of each standard curve. Primer amplification efficiency (E) was calculated as:

$$E = 10^{\left(\frac{-1}{slope}\right)} - 1$$

Efficiencies between 90 % to 110 % were considered acceptable, in accordance with established RT-qPCR quality criteria (Rogers-Broadway & Karteris, 2015).

2.2.5.2 Melting Curve Analysis

Amplification specificity was confirmed by melting curve analysis. Fluorescence was continuously monitored while the temperature was gradually increased to induce denaturation of double-stranded PCR products. A single, well-defined peak at the expected gene-specific melting temperature confirms the absence of non-specific amplification products and primer-dimer formation (Tolvanen & Karp, 2011). A representative melting curve for *TBP* is shown in Figure 7.

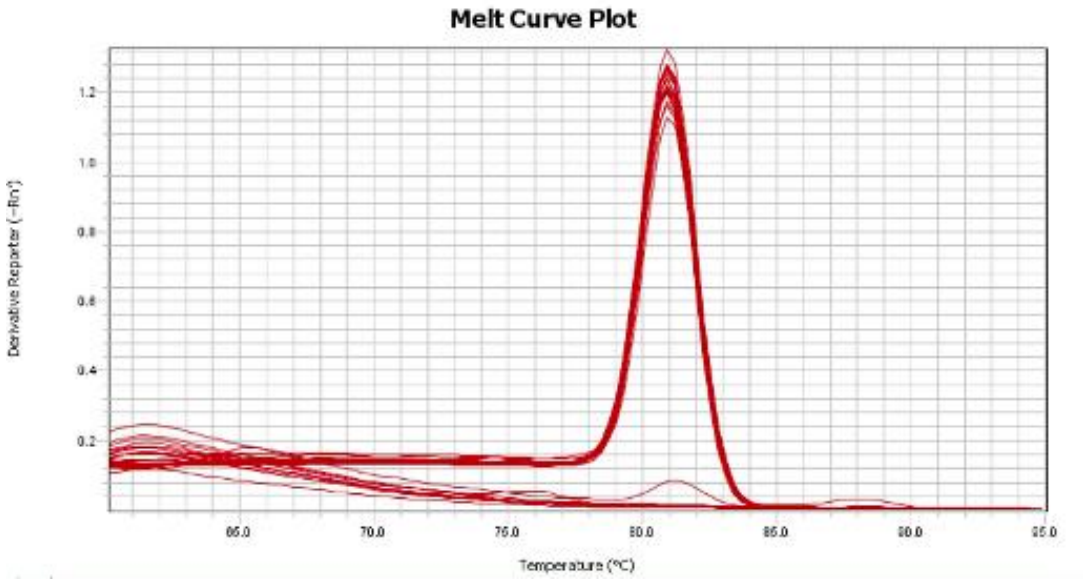

Figure 7: Representative melting curve of the housekeeping gene TATA binding protein (TBP), illustrating the assessment of amplification specificity. *During the melting curve analysis, the PCR product is gradually heated, causing the double-stranded DNA to denature and release the fluorescent dye, resulting in a drop in fluorescence signal. The y-axis displays the rate of this fluorescence, which produces a characteristic peak at the melting temperature of the amplicon. The single, well-defined peak confirms the presence of one specific amplification product with no detectable non-specific byproducts or primer-dimer formations [QuantStudio™ 6 Flex].*

2.2.5.3 Agarose Gel Electrophoresis

To further validate primer specificity and confirm amplicon size, agarose gel electrophoresis was performed. This method allows direct visualization of PCR products and verification of expected fragment length by separating DNA fragments based on their molecular weight.

A 1 x TAE running buffer was prepared by diluting 10 mL of 50 x TAE buffer (Thermo Fisher Scientific) in 500 mL deionized water. Agarose gels were prepared by dissolving 2 g agarose in 110 mL diluted TAE buffer, followed by heating until complete dissolution. After cooling for approximately 10 minutes, 5 µL of peqGreen DNA stain (peqlab) was added as a fluorescent dye while stirring the solution on a magnetic stirrer. The solution was poured into a 2D electrophoresis chamber, covered and allowed to solidify for approximately 30 minutes.

5 µL of GeneRuler 100 bp DNA Ladder (Thermo Fisher Scientific) was loaded into the first lane as a molecular weight reference. PCR products were mixed with 1 µL 6 x DNA Loading Dye and loaded into the subsequent wells. Electrophoresis was performed at 88 V until adequate separation was achieved. Bands were visualized using a ChemiDoc imaging system (Bio-Rad), allowing confirmation of primer specificity based on the presence of single bands at the expected amplicon size.

2.2.6 RT-qPCR

Following primer validation, RT-qPCR was performed for all target genes using technical duplicates in a 384-well plate format. cDNA samples were diluted 1:4 with NF-H_2O prior to analysis. Each reaction contained a total volume of 10 µL, consisting of 3 µL primer mix, 1 µL diluted cDNA, 1 µL NF-H_2O and 5 µL of ChamQ SYBR qPCR Master Mix (Vazyme).

Non-template controls (NTCs) were prepared in duplicate for each primer pair in every run by replacing the cDNA with 1 µL NF-H_2O to assess potential contamination or non-specific amplification. Plates were centrifuged at 400 rpm for 20 seconds and subsequently loaded into the QuantStudio™ 6 Flex RT-PCR system (Thermo Fisher Scientific). The heated lid was set to 105 °C prior to run. Thermal cycling conditions followed a standardized RT-qPCR program, as illustrated in Figure 8.

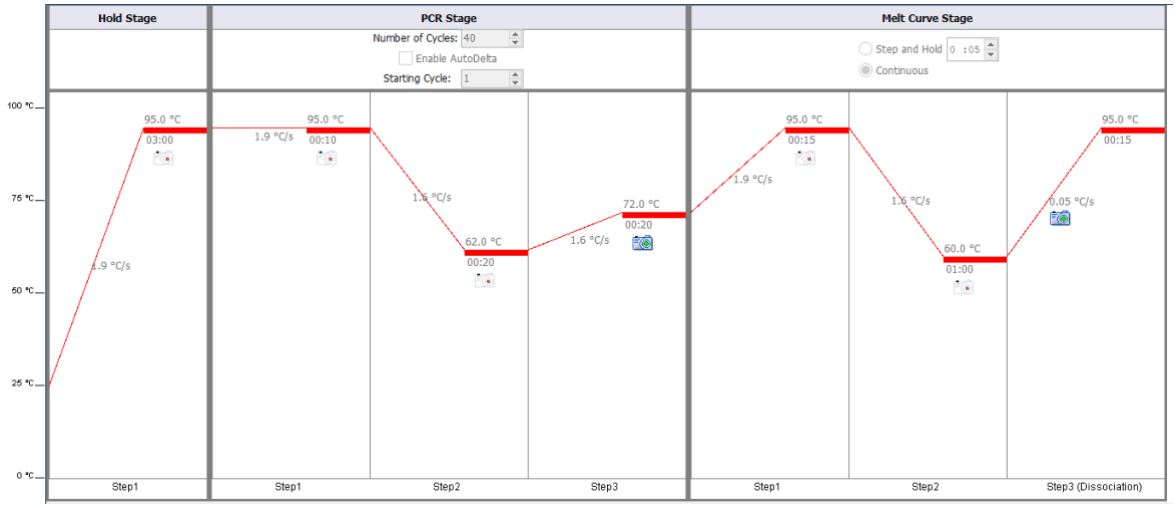

Figure 8: Display of the thermal cycling conditions applied for RT-qPCR analysis using the QuantStudio™6 Flex RT-PCR system. *The program consists of distinct stages, each corresponding to specific temperature and time settings required for efficient cDNA amplification and fluorescence detection [QuantStudio™ 6 Flex].*

Data analysis was performed using QuantStudio™ real-time PCR Software v1.6.1. Amplification plots were generated by plotting fluorescence intensity against cycle number. Ct values were determined using a uniform threshold applied across all runs. Raw data were exported to Microsoft Excel™. A representative amplification plot for *ACADM* expression in murine liver tissue is shown in Figure 9.

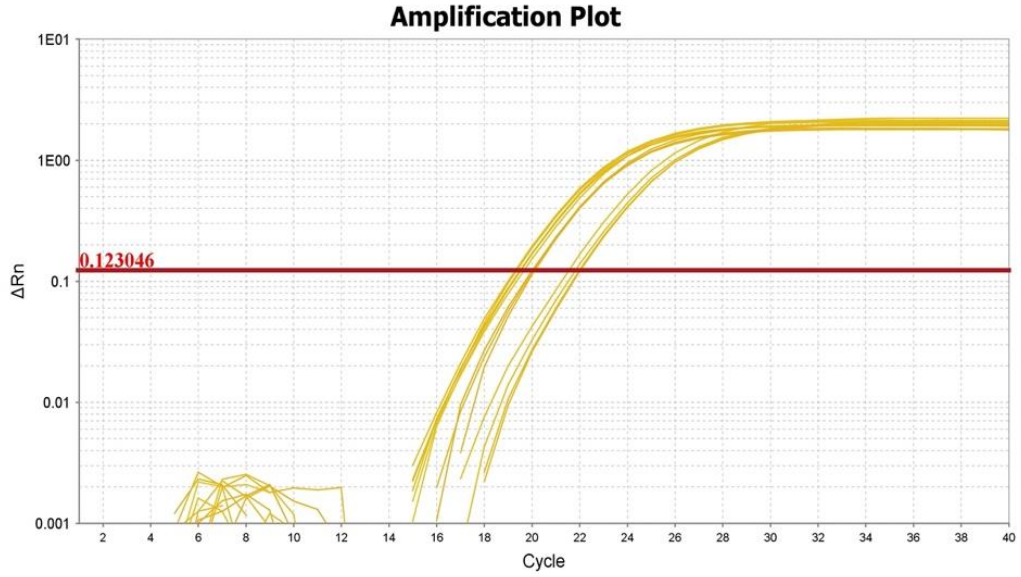

Figure 9: Representative amplification plot of acyl-CoA dehydrogenase medium-chain (ACADM) expression in murine liver tissue, generated by the QuantStudio™ 6 Flex. *The y-axis displays the normalized reporter signal (ΔRn), calculated as the fluorescence intensity of the reporter dye minus the baseline signal, plotted on a logarithmic scale against the PCR cycle number. In this study SYBR Green served as the reporter dye. The horizontal line indicates the fluorescence threshold, set uniformly across all runs. The cycle at which each sample's amplification curve crosses this threshold defines the cycle threshold (Ct) value [QuantStudio™ 6 Flex].*

2.3 Statistics

Statistical analyses were performed using GraphPad Prism version 7 (GraphPad Software, San Diego, CA, USA). Relative messenger ribonucleic acid (mRNA) expression levels were calculated using the $2^{-\Delta Ct}$ method, with normalization to the mean of the two HKGs *TBP* and *Rpl4*, which showed comparable expression stability across all samples. In addition, consistent Ct threshold settings were applied across all plates to minimize technical variability and ensure comparability between conditions.

To assess differences between experimental groups, data were first evaluated for normal distribution. For normally distributed data, a one-way analysis of variance (ANOVA) was applied. In cases where normality assumptions were not met, the Kruskal-Wallis test was used. Dunn's multiple comparisons test was performed for post hoc analysis to identify significant differences between individual groups. Outliers were identified through Grubbs' test. A significance level of $\alpha = 0.05$ was applied throughout.

Results are presented as box-and-whisker plots, in which the box represents the interquartile range (25^{th}-75^{th} percentile), the central line indicates the median and whiskers show the minimum and maximum values.

Statistical significance is indicated as: *$p \leq 0.05$, **$p \leq 0.01$, ***$p \leq 0.001$.

3. Results

The expression of selected target genes involved in lipid metabolism and mitochondrial function was analyzed in cardiac and hepatic tissue from mice subjected to different dietary conditions: SD, LCT-enriched KD, LCT/MCT-enriched KD, IF and CR.

3.1 Primer Efficiency via RT-qPCR

Primer performance was assessed by generating standard curves from a 1:3 serial dilution of a previously 1:10-diluted cDNA working stock, as described in section 2.2.5.1. Ct values from the RT-qPCR analysis were plotted against the logarithm of the cDNA concentration and linear regression analysis was performed to assess amplification efficiency. Primer efficiency was calculated based on the slope of each regression line using the formula described in section 2.2.5.1.

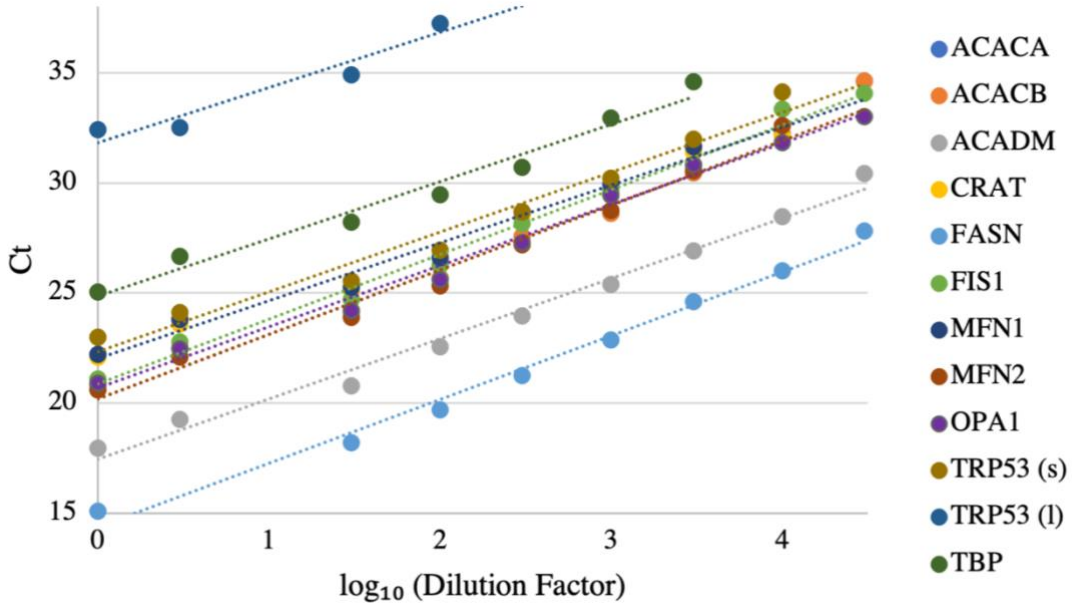

Figure 10: Standard curves for primer efficiency assessment. *Standard curves were generated from a 1:3 serial dilution of a previously 1:10 diluted cDNA working solution. For each primer pair, the cycle threshold (Ct) values obtained from RT-qPCR were plotted against the logarithm of the cDNA concentration. All curves demonstrated high linearity ($R^2 > 0.95$), indicating consistent and specific amplification across the tested concentration range. ACACA Acetyl-CoA carboxylase alpha; ACACB Acetyl-CoA carboxylase beta; ACADM Acyl-CoA dehydrogenase medium-chain; CRAT Carnitine O-acetyltransferase; FASN Fatty acid synthase; FIS1 Mitochondrial fission protein 1; MFN1 Mitofusin 1; MFN2 Mitofusin 2; OPA1 Optic atrophy protein 1; RT-qPCR Reverse transcription quantitative polymerase chain reaction; TBP TATA box binding protein; Trp53 (long) Tumor protein p53, long isoform; Trp53 (short) Tumor protein p53, short isoform.*

As shown in Figure 10, all primer pairs demonstrated high linearity across the tested dilution range ($R^2 > 0.95$). Calculated efficiencies ranged from 90 % to 108 %, falling within the accepted range for RT-qPCR analysis (Rogers-Broadway & Karteris, 2015).

Detailed efficiency values for each primer pair are provided in Table 3 (Section 2.1.3). These results confirm reliable amplification behavior and suitability of all selected primer pairs for downstream gene expression analysis.

3.2 Primer Validation via Gel Electrophoresis

Primer specificity and amplicon size were further validated by agarose gel electrophoresis. As shown in Figure 11, all primer pairs produced bands at positions consistent with the expected amplicon sizes, as estimated by comparison with the GeneRuler 100 bp DNA ladder (lane 1).

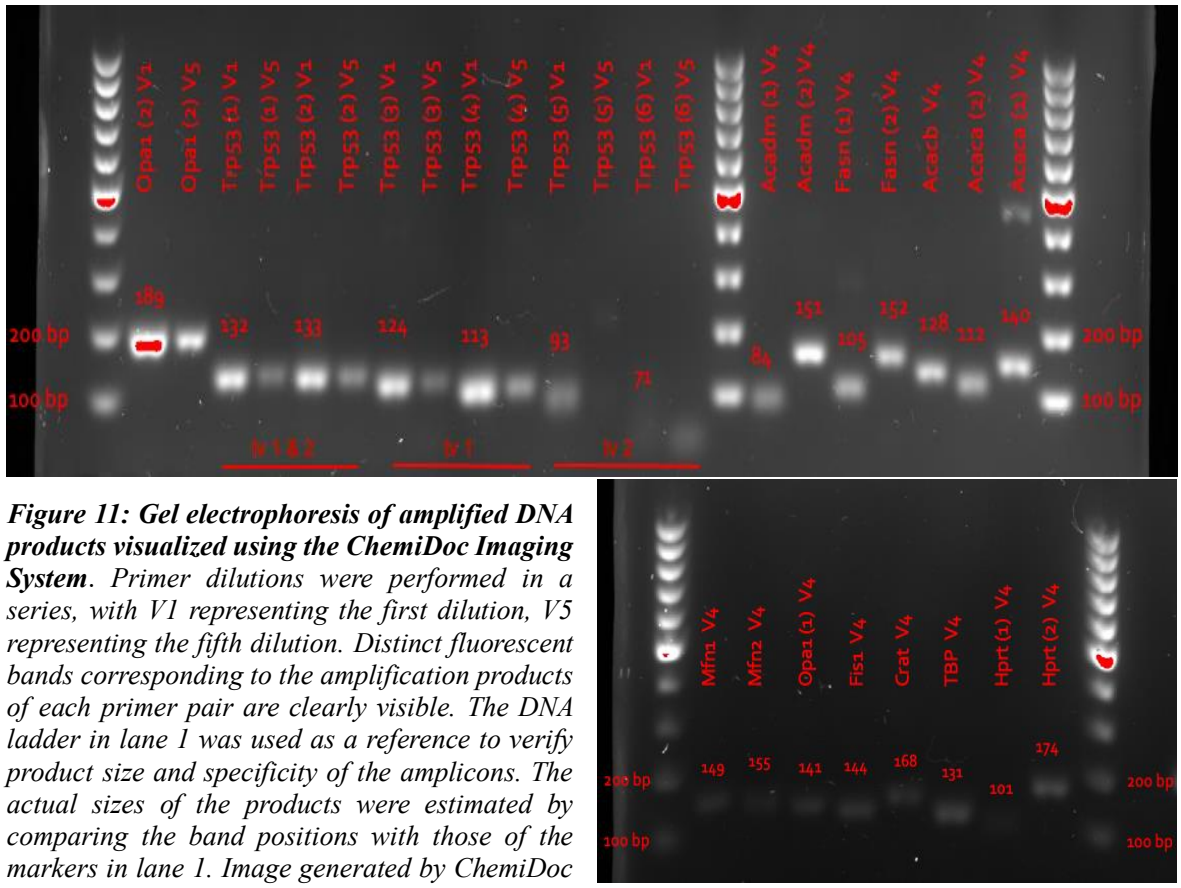

Figure 11: Gel electrophoresis of amplified DNA products visualized using the ChemiDoc Imaging System. *Primer dilutions were performed in a series, with V1 representing the first dilution, V5 representing the fifth dilution. Distinct fluorescent bands corresponding to the amplification products of each primer pair are clearly visible. The DNA ladder in lane 1 was used as a reference to verify product size and specificity of the amplicons. The actual sizes of the products were estimated by comparing the band positions with those of the markers in lane 1. Image generated by ChemiDoc (Bio-Rad). ACACA Acetyl-CoA carboxylase alpha; ACACB Acetyl-CoA carboxylase beta; ACADM Acyl-CoA dehydrogenase medium-chain; CRAT Carnitine O-acetyltransferase; FASN Fatty acid synthase; FIS1 Mitochondrial fission protein 1; MFN1 Mitofusin 1; MFN2 Mitofusin 2; OPA1 Optic atrophy protein 1; RT-qPCR Reverse transcription quantitative polymerase chain reaction; TBP TATA box binding protein; Trp53 (long) Tumor protein p53, long isoform; Trp53 (short) Tumor protein p53, short isoform; Tv Transcript Variant.*

To identify the most suitable primer design for each target gene, multiple primer variants were evaluated. This was particularly relevant for genes including *ACACA*, *ACADM*, *FASN*, *OPA1*, *Trp53* and the HGK hypoxanthine-guanine phosphoribosyltransferase (*HPRT*), which was used within the same experimental framework. The variant showing the sharpest band at the expected fragment size was selected for further analysis. In the

case of *ACADM*, two variants generated amplicons of approximately 84 bp and 151 bp, respectively. The primer pair generating the longer amplicon was selected for subsequent analyses due to its sharper band appearance.

For *Trp53*, several primer variants were evaluated. Certain variants produced weak or diffuse bands without a clearly defined amplicon, indicating insufficient amplification efficiency. These primer sets were therefore excluded from further analyses.

Primer dilutions were tested in a serial format (V1-V5), with V1 representing the highest and V5 the most diluted primer concentration, enabling the assessment of amplification robustness across a range of primer concentrations. Single bands at the expected positions indicated primer specificity and the absence of non-specific amplification products.

3.3 Effects of Dietary Interventions on Body Weight Development and Adipose Tissue Mass

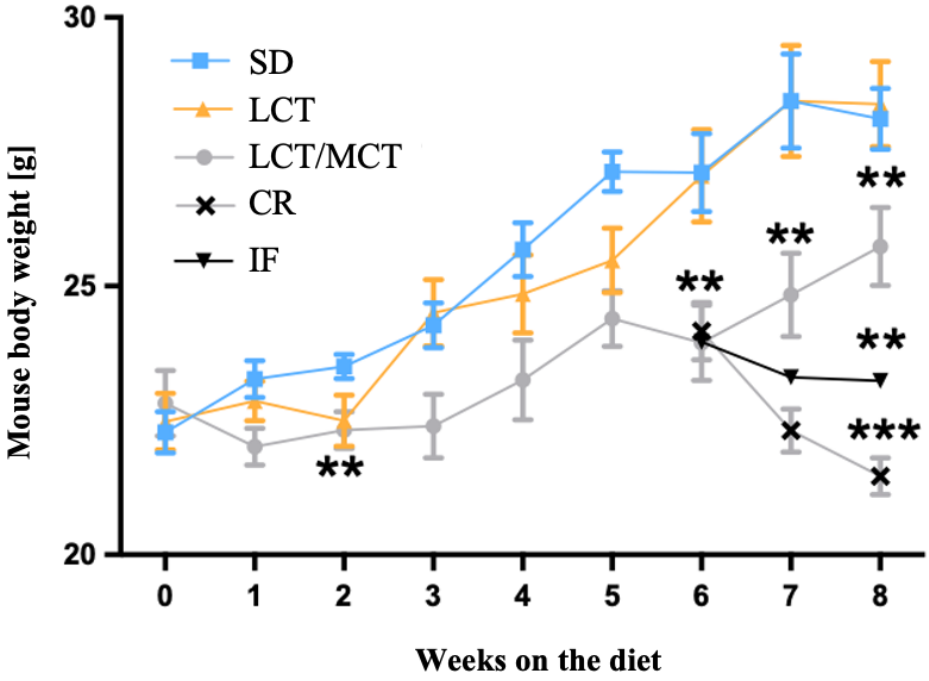

Figure 12: Body weight progression of mice over the dietary intervention period. *Animals were assigned to one of five dietary groups: Standard diet (SD), long-chain triglyceride ketogenic diet (LCT), combined long- and medium-chain triglyceride ketogenic diet (LCT/MCT), intermittent fasting (IF) or calorie restriction (CR). SD, LCT and LCT/MCT groups were maintained for 8 weeks, whereas IF and CR interventions started in the final two weeks of the intervention. SD- and LCT-fed mice showed a continuous increase in body weight, whereas CR and IF resulted in a decline. LCT/MCT diet induced a less pronounced body weight gain. Body weight [g] was measured weekly and is presented as mean ± standard error. Statistical significance relative to SD is indicated as: **$p \leq 0.01$, ***$p \leq 0.001$ [Adapted from Sternberg et al. (2023)].*

As shown in Figure 12, body weight diverged between dietary groups over the intervention period. SD- and LCT-fed mice showed a continuous increase in body mass over the observation period, while weight gain was less pronounced in the LCT/MCT group. Both energy-restricted conditions led to reduced body weight relative to SD, with CR showing a decline at later time points, whereas IF induced a comparatively milder reduction. These findings indicate that both dietary fat composition and caloric availability influence body weight regulation.

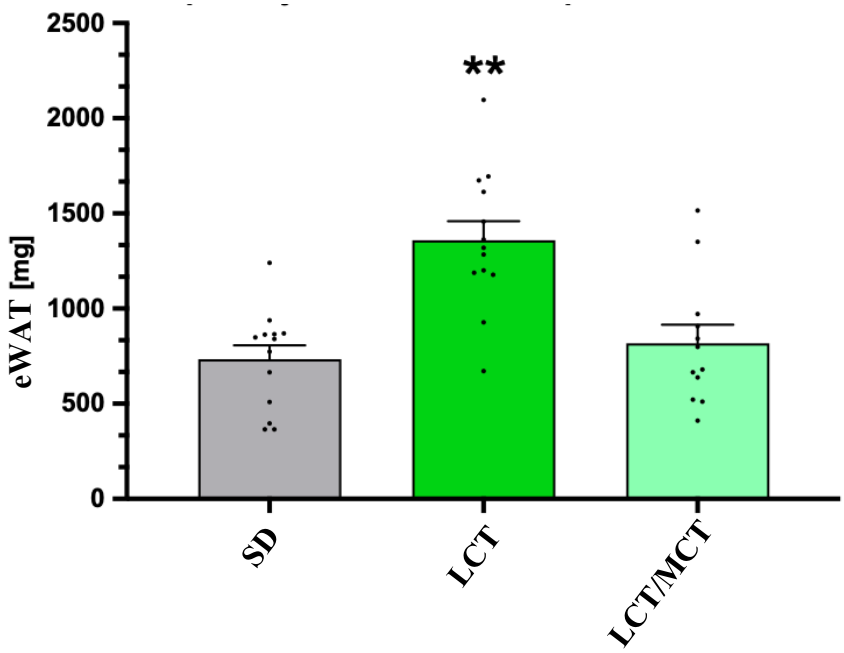

Figure 13: Epididymal white adipose tissue (eWAT) mass at the end of the dietary intervention. *eWAT mass [mg] was determined at the end of the intervention period. Individual data points represent single animals. Long-chain triglyceride (LCT) ketogenic diet resulted in a significant increase in eWAT mass compared to standard diet (SD), whereas eWAT mass in the combined long-chain and medium-chain triglyceride (LCT/MCT) ketogenic diet remained comparable to SD levels. Statistical significance relative to SD is indicated as: **$p \leq 0.01$ [Adapted from Sternberg et al.].*

To further characterize the effects of dietary fat composition on adipose tissue, epididymal white adipose tissue (eWAT) mass was assessed at the end of the intervention period (Figure 13). LCT-fed mice showed a significant increase in eWAT mass compared to SD, indicating pronounced visceral lipid accumulation under KD without MCTs. In contrast, eWAT mass in the LCT/MCT group remained comparable to SD and did not differ significantly from it, suggesting that the partial replacement of LCFAs with MCFAs attenuated the accumulation of visceral adipose tissue seen under pure LCT feeding.

3.4 Gene Expression in Cardiac Tissue

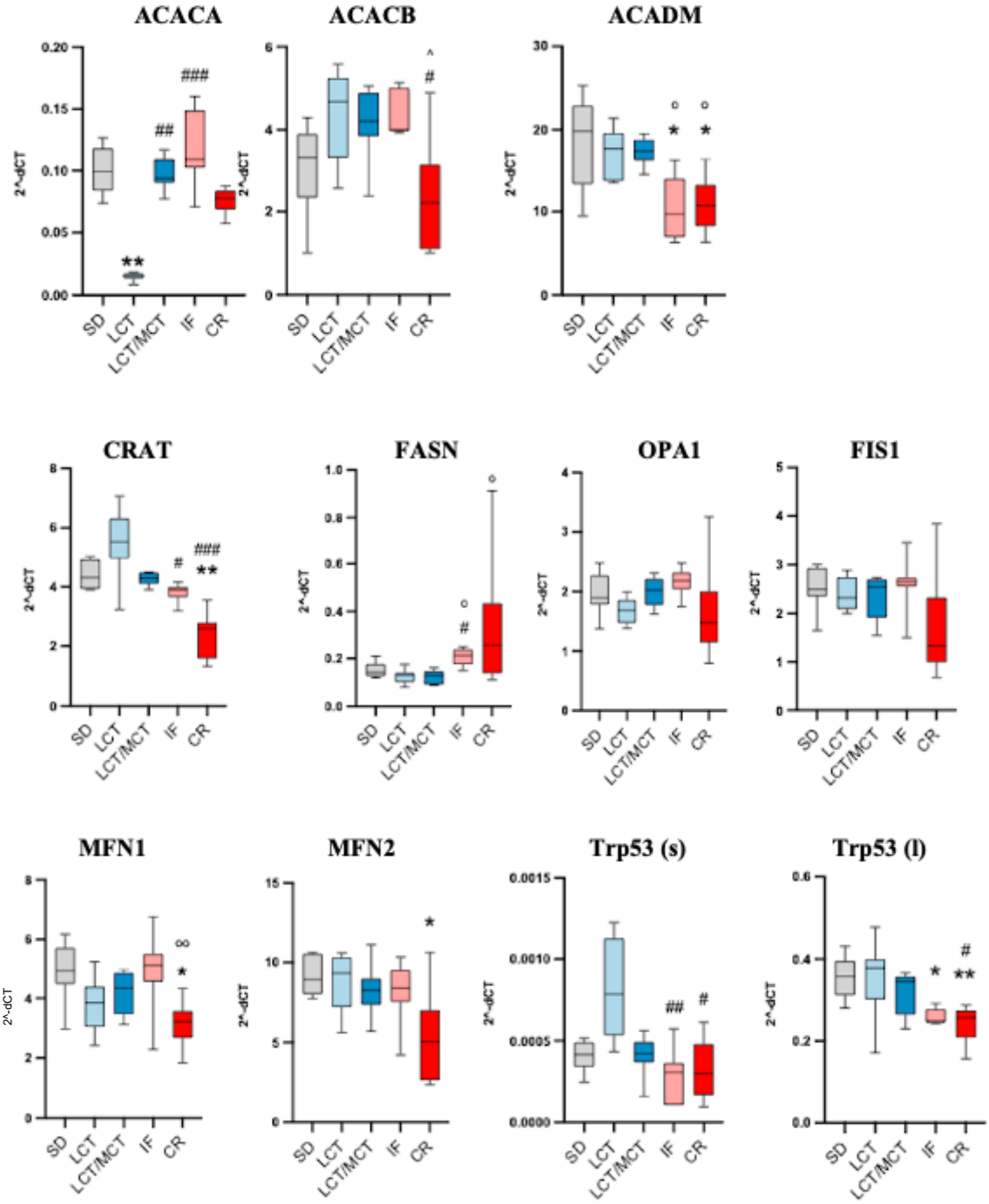

Figure 14: Cardiac gene expression profiles under different dietary interventions. *Relative mRNA expression levels of ACACA, ACACB, ACADM, MFN1, CRAT, FASN, OPA1, FIS1, MFN2, Trp53 (s) and Trp53 (l), were analyzed in heart tissue of mice fed SD, LCT, LCT/MCT, IF or CR diets. Gene expression was assessed by RT-qPCR and normalized to the geometric mean of the housekeeping genes Rpl4 and TBP. Data represented as $2^{-\Delta Ct}$ values. *p ≤ 0.05, **p ≤ 0.01, ***p ≤ 0.001 versus SD, # versus LCT, ° versus LCT/MCT, ^ versus IF, One-way ANOVA. ACACA Acetyl-CoA carboxylase alpha; ACACB Acetyl-CoA carboxylase beta; ACADM Acyl-CoA dehydrogenase medium-chain; CR Calorie restriction; CRAT Carnitine O-acetyltransferase; FASN Fatty acid synthase; FIS1 Mitochondrial fission protein 1; IF Intermittent fasting; LCT Long-chain triglyceride; LCT/MCT Long-chain and medium-chain triglyceride; MFN1 Mitofusin 1; MFN2 Mitofusin 2; OPA1 Optic atrophy protein 1; RT-qPCR Reverse transcription quantitative polymerase chain reaction; Rpl4 Ribosomal protein L4; SD Standard diet; TBP TATA box binding protein; Trp53 (l) Tumor protein p53, long isoform; Trp53 (s) Tumor protein p53, short isoform.*

Gene expression analysis in cardiac tissue covered pathways of lipid metabolism, mitochondrial dynamics and cellular stress signaling (Figure 14).

3.4.1 Ketogenic Diets Have Limited Effects on Lipogenic Gene Expression

KDs induced distinct transcriptional changes in cardiac tissue, primarily affecting genes involved in lipogenesis.

ACACA expression was significantly reduced under LCT feeding compared to SD, representing the most pronounced transcriptional change observed under ketogenic conditions. This suppression was specific to LCT, as *ACACA* expression under LCT/MCT feeding did not differ significantly from SD, indicating a less pronounced lipogenic response under the combined lipid diet.

ACACB expression remained relatively stable across all dietary groups. While no significant differences were observed between SD and KDs, a significant difference was detected between CR and LCT, with lower *ACACB* transcript levels under CR.

The expression of *FASN* did not differ significantly from SD under either KD, further indicating that cardiac lipogenic gene expression is largely unresponsive to ketogenic feeding.

ACADM expression remained stable under both LCT and LCT/MCT conditions and did not differ significantly from SD. This stability suggests that medium-chain FAO capacity in cardiac tissue was not further transcriptionally induced by KDs.

3.4.2 Coordinated Transcriptional Downregulation of Oxidative Pathways under Energy Restriction

Under CR and IF, cardiac gene expression showed a coordinated transcriptional downregulation of genes involved in mitochondrial FAO and acetyl-CoA handling.

The expression of *ACADM*, which is inherently high in the heart, was significantly reduced under both CR and IF compared to SD. Similarly, *CRAT* showed a lower expression in the CR group. The parallel suppression of these functionally linked genes points to a transcriptional reduction of mitochondrial β-oxidation capacity.

In parallel, the expression of *FASN* showed a divergent pattern. IF was associated with a significant increase relative to both LCT and LCT/MCT and CR showed significant higher levels compared to LCT/MCT, though neither of the energy-restricted groups differed significantly from SD.

3.4.3 Mitochondrial Dynamics Genes Show Limited but Energy-Dependent Variation

Genes regulating mitochondrial fusion and fission showed limited variation in transcriptional expression, indicating that overall mitochondrial network integrity was largely preserved across dietary interventions.

Under CR, expression of both *MFN1* and *MFN2* were significantly reduced relative to SD. This reduction occurred alongside decreased expression of *ACADM* and *CRAT*, suggesting a broader coordinated downregulation of mitochondrial gene programs under CR rather than an isolated change in network dynamics.

In contrast, expression of *FIS1* and *OPA1* remained stable across all dietary groups. Overall, KDs diets did not significantly alter the expression of any mitochondrial dynamics gene. The stability of *MFN1*, *MFN2*, *FIS1* and *OPA1* under these conditions indicates that increased dietary lipid availability did not affect transcriptional regulation of mitochondrial network remodeling in cardiac tissue.

3.4.4 Stress-Related Trp53 Expression Is Reduced under Energy Restriction

Trp53 long and short isoforms differed in expression level and diet-dependent regulation. Across all dietary groups, the long isoform was expressed at markedly higher levels than the short isoform, confirming it as the predominant *Trp53* transcript in cardiac tissue.

Under both CR and IF, the expression of the long isoform was significantly reduced compared to SD. KDs did not induce significant changes in either isoform. The short isoform remained at consistently low levels, with a downward trend under CR and IF that did not reach statistical significance compared to SD, but to LCT.

The absence of significant *Trp53* changes under LCT and LCT/MCT feeding indicates that high lipid availability did not trigger a transcriptional stress response in cardiac tissue under the conditions of this study. The reduced *Trp53* expression under energy restriction, predominantly affecting the long isoform, suggests that calorie limitation, rather than dietary fat composition, is the primary driver of stress-associated transcriptional changes in the heart.

3.5 Gene Expression in Hepatic Tissue

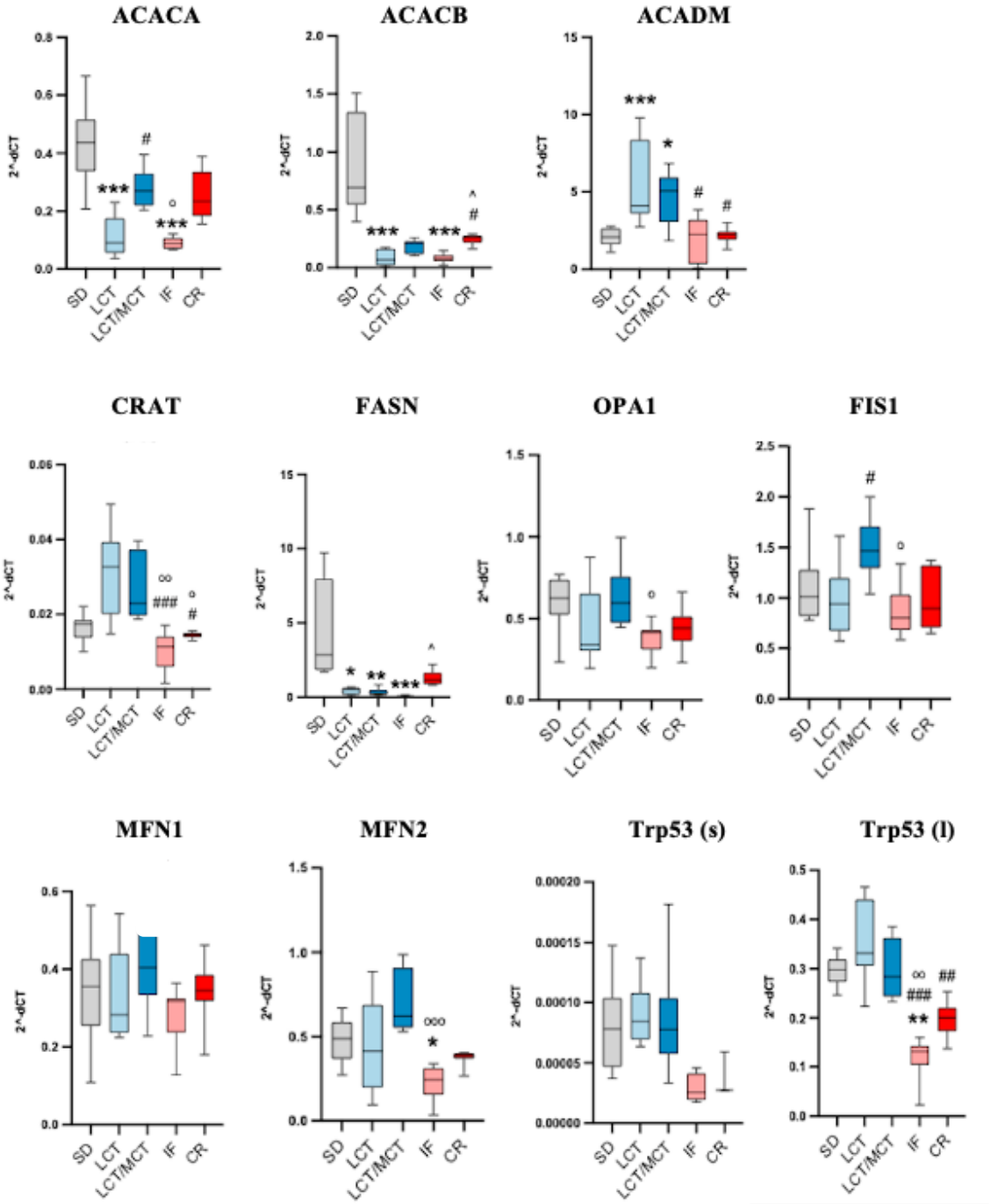

Figure 15: Hepatic gene expression profiles under different dietary interventions. *Relative mRNA expression levels of ACACA, ACACB, ACADM, MFN1, CRAT, FASN, OPA1, FIS1, MFN2, Trp53 (s) and Trp53 (l), were analyzed in liver tissue of mice fed SD, LCT, LCT/MCT, IF or CR diets. Gene expression was assessed by RT-qPCR and normalized to the geometric mean of the housekeeping genes Rpl4 and TBP. Data represented as $2^{-\Delta Ct}$ values. *p ≤ 0.05, **p ≤ 0.01, ***p ≤ 0.001 versus SD, # versus LCT, ° versus LCT/MCT, ^ versus IF, One-way ANOVA. ACACA Acetyl-CoA carboxylase alpha; ACACB Acetyl-CoA carboxylase beta; ACADM Acyl-CoA dehydrogenase medium-chain; CR Calorie restriction; CRAT Carnitine O-acetyltransferase; FASN Fatty acid synthase; FIS1 Mitochondrial fission protein 1; IF Intermittent fasting; LCT Long-chain triglyceride; LCT/MCT Long-chain and medium-chain triglyceride; MFN1 Mitofusin 1; MFN2 Mitofusin 2; OPA1 Optic atrophy protein 1; RT-qPCR Reverse transcription quantitative polymerase chain reaction; Rpl4 Ribosomal protein L4; SD Standard diet; TBP TATA box binding protein; Trp53 (l) Tumor protein p53, long isoform; Trp53 (s) Tumor protein p53, short isoform.*

Given the liver's central role in lipid handling and ketone body production, distinct transcriptional responses to the dietary interventions were expected. Gene expression analysis covered pathways of lipid metabolism, mitochondrial organization and cellular stress signaling (Figure 15).

3.5.1 Coordinated Suppression of Lipogenic Genes under Ketogenic Diets and Fasting

Genes involved in hepatic lipogenesis were broadly downregulated under both KDs and IF.

ACACA expression was significantly reduced under LCT feeding and IF compared to SD. A downward trend was also observed under LCT/MCT and CR, although these did not reach statistical significance.

ACACB followed a comparable pattern, showing significantly lower expression under LCT and IF relative to SD and non-significant reductions under LCT/MCT and CR. The parallel regulation of both *ACACA* and *ACACB* indicates a coordinated reduction in hepatic malonyl-CoA-producing capacity under high lipid availability and intermittent energy restriction.

Consistent with this pattern, *FASN* expression was markedly reduced in the LCT, LCT/MCT and IF groups compared to SD. Under CR, *FASN* levels were significantly higher than under IF, yet remained below SD. The expression of *ACACA*, *ACACB* and *FASN* demonstrate that both dietary lipid oversupply and IF are associated with broad downregulation of hepatic DNL, whereas CR induces a comparatively moderate transcriptional response.

3.5.2 Upregulation of Hepatic Fatty Acid Oxidation Capacity under Ketogenic Diets

Genes involved in mitochondrial β-oxidation and acetyl-CoA transfer showed distinct, diet-specific expression patterns in the liver.

ACADM expression was significantly upregulated under both LCT and LCT/MCT feeding compared to SD, indicating an enhanced transcriptional capacity for FAO in response to increased lipid availability. Under IF and CR, *ACADM* levels did not differ significantly from SD, suggesting that energy restriction per se did not additionally affect hepatic FAO gene expression under these conditions.

The expression of *CRAT* was significantly reduced under IF and CR compared to both KDs. Under LCT and LCT/MCT feeding, *CRAT* levels tended to be higher than under SD, though this difference was not statistically significant. This pattern may indicate a selective downregulation of acetyl-CoA buffering capacity under energy-restricted conditions, while KDs were associated with relatively preserved *CRAT* expression.

3.5.3 Mitochondrial Dynamics Genes Remain Largely Stable Across Diets

Genes regulating mitochondrial fusion and fission showed limited transcriptional variability in hepatic tissue, indicating overall stability of mitochondrial structural regulation across dietary conditions.

MFN1 expression did not differ significantly across the diet groups. *MFN2* levels remained largely stable, except for a significant reduction under IF compared to SD and LCT/MCT. *OPA1* and *FIS1* expression did not differ from SD levels under any condition but were both significantly reduced under IF relative to LCT/MCT. Additionally, *FIS1* expression was significantly higher under LCT/MCT than under LCT, suggesting that the combined lipid source may mildly promote transcriptional activity associated with mitochondrial remodeling.

The mild IF-associated downregulation of *MFN2, OPA1* and *FIS1* may point toward a selective attenuation of mitochondrial dynamics gene expression during fasting.

3.5.4 Energy Restriction Suppresses Hepatic Trp53 Expression

Hepatic *Trp53* expression showed diet-dependent regulation, primarily driven by energy-restriction. The long isoform was significantly reduced under IF compared to SD, LCT and LCT/MCT, and was also significantly lower under CR relative to LCT.

The short isoform was expressed at markedly lower levels across all dietary conditions, confirming the long isoform as the dominant hepatic *Trp53* transcript. Although no statistically significant differences between the groups were observed for the short isoform, a downward trend showed under IF and CR.

The *Trp53* expression remained stable under both KDs in both isoforms compared to SD.

4. Discussion

The present study shows that dietary fat composition and energy availability shape gene expression related to lipid metabolism and mitochondrial function differentially depending on the tissue. Liver and heart both rely on mitochondrial function, but their transcriptional responses to KDs and energy restriction differed markedly. This reflects their fundamentally different metabolic roles.

4.1 Overview of Tissue-Specific Metabolic Adaptations

The central question of this study was whether LCT and LCT/MCT KDs, despite their comparable total lipid content, produce distinct transcriptional adaptations in cardiac and hepatic tissue. The data show that the two diets are not equivalent at the transcriptional level and that the tissue is a primary factor of the observed responses (Figure 16).

This metabolic difference is not only reflected at the transcriptional level but is also visible at the phenotype: LCT-fed mice showed a significant increase in eWAT mass compared to SD, while the LCT/MCT group remained at comparable levels to SD (Figure 13). This is consistent with the rapid hepatic oxidation of MCFAs which may reduce the availability for peripheral lipid storage (Bach et al., 1989; Papamandjaris et al., 1998).

In the heart, transcriptional changes under KDs were comparatively modest, particularly for genes involved in FAO and mitochondrial dynamics. This is in line with the metabolic profile of the adult heart, which already relies predominantly on LCFA oxidation under basal conditions. The heart may therefore have limited additional transcriptional flexibility in response to further increased lipid supply. In contrast, the liver, as the central regulator of systemic lipid handling and ketone body production, was more transcriptionally responsive to changes in dietary fat content by suppressing lipogenic genes and upregulating FAO capacity. Notably, several differences between LCT and LCT/MCT feeding were observed, suggesting that the inclusion of MCFAs alters hepatic metabolic signaling beyond the effect of high fat intake alone.

Energy-restriction produced different transcriptional responses. In the heart, CR was associated with a coordinated downregulation of genes involved in FAO, mitochondrial fusion and *Trp53*, pointing to a broad transcriptional shift toward energy conservation. IF produced a similar picture, primarily affecting *ACACDM* and *Trp53.* In the liver, IF caused the most pronounced suppression in lipogenic gene expression. CR induced comparatively stable hepatic transcriptional level.

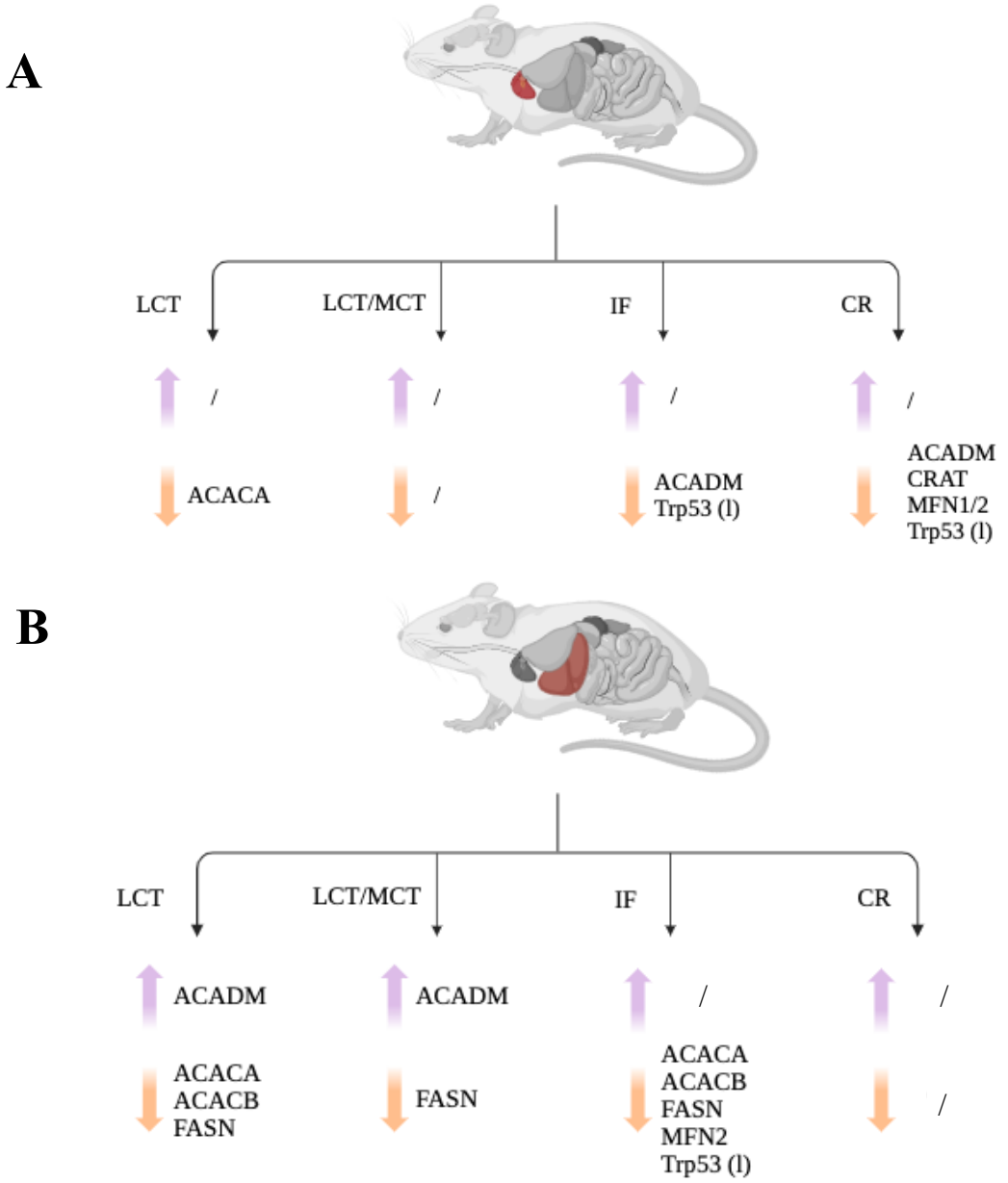

Figure 16: Overview of significant relative gene expression changes in murine heart and liver following dietary interventions compared to standard diet (SD). *(A) Cardiac gene expression remained comparatively stable across ketogenic diets (KD), (B) while hepatic tissue showed stronger transcriptional responses to differences in dietary fat composition. (A-B) Energy restriction was associated with coordinated downregulation of oxidative and stress-related pathways. / = no significant alteration compared to SD. ACACA Acetyl-CoA carboxylase alpha; ACACB Acetyl-CoA carboxylase beta; ACADM Acyl-CoA dehydrogenase medium-chain; CR Calorie restriction; CRAT Carnitine O-acetyltransferase; FASN Fatty acid synthase; IF Intermittent fasting; LCT Long-chain triglyceride ketogenic diet; LCT/MCT Long-chain and medium-chain triglyceride ketogenic diet; MFN1 Mitofusin 1; MFN2 Mitofusin 2; Trp53 (l) Tumor protein p53, long isoform [Created by author using BioRender.com].*

Taken together, these findings point toward a complementary relationship between the two organs: While the liver flexibly adapts its transcriptional expression to regulate energy availability, the heart appears to maintain transcriptional stability under changing nutritional conditions.

4.2 Regulation of Lipogenic Gene Expression in Response to Dietary Fat Composition

The following section addresses the regulation of central lipogenic genes, focusing on how dietary fat composition may differentially influence liver and heart tissue.

4.2.1 Heart

The expression of lipogenic genes changed less in the heart than in the liver, consistent with the heart's limited capacity for DNL. Nevertheless, subtle differences between dietary groups were observed.

ACACA expression was significantly reduced under LCT feeding, while it remained comparable to SD under LCT/MCT. Given the heart's limited capacity for DNL, ACC1 in cardiac tissue may serve a different role than in the liver, potentially contributing more to malonyl-CoA-mediated CPT1 regulation than to fatty acid synthesis. If so, the suppression of *ACACA* under LCT could reflect a reduced need for CPT1 inhibition when LCFA oxidation is the primary pathway. However, this hypothesis remains speculative as there is no correlation to protein data and/or enzymatic activity included in the analysis.

The lack of *ACACA* suppression under LCT/MCT may be explained by the more rapid oxidation of MCTs. Although MCTs in cardiac tissue appear to remain CPT1-dependent (Pereyra et al., 2023), their faster oxidation relative to LCTs may reduce the overall demand for malonyl-CoA mediated regulation of mitochondrial fatty acid entry and with this, the need to suppress *ACACA* transcription. This would suggest that it is not the independence from CPT1, but rather the metabolic efficiency of MCFA oxidation. It should be noted that the specific role of ACC1 in CPT1 regulation under KDs is poorly studied.

The expression of *ACACB* remained stable across all dietary groups compared to SD, in contrast to the liver where it was suppressed under LCT. This likely reflects the difference in how the two tissues regulate mitochondrial fatty acid entry. In the liver, where CPT1A has relatively moderate malonyl-CoA sensitivity, the transcriptional downregulation of *ACACB* is needed to reduce malonyl-CoA and relieve CPT1 inhibition. In the heart, CPT1B is approximately 100-fold more sensitive to malonyl-CoA inhibition, meaning that even small reductions in malonyl-CoA are sufficient to increase fatty acid uptake (Schreurs et al., 2010).

FASN did not change significantly under KDs. Cardiac *FASN* may serve functions beyond DNL, such as contributing to calcium handling (Razani et al., 2011). This could explain why it does not respond to dietary fat composition in the same way as the liver. However, whether ketogenic conditions specifically influence cardiac *FASN* expression remains poorly studied.

4.2.2 Liver

The hepatic transcriptional expression of *ACACA*, *ACACB* and *FASN* generally showed a coordinated downward trend, with the most pronounced reductions observed in the LCT and IF groups.

The suppression of all three lipogenic genes under LCT feeding fits the classical hepatic response to high LCFA availability: Reduced insulin signaling activates AMPK, which phosphorylates and inhibits both ACC1 and ACC2, thereby reducing malonyl-CoA production and favoring mitochondrial FAO over lipid synthesis (Galic et al., 2018; Rui, 2014). Under LCT/MCT feeding, this anti-lipogenic transcriptional response was attenuated, particularly *ACACA* and *ACACB* did not reach statistical significance relative to SD. This may reflect the different hepatic pathway of MCFAs: Their rapid uptake and preferential oxidation may reduce intracellular lipid accumulation and thereby dampen the feedback signals that normally influence lipogenic gene suppression.

It's also worth noting that previous studies have shown that under ketogenic conditions, ACC1 activity can be regulated through post-translational mechanisms. Phosphorylation and malonylation of ACC1 can modulate enzyme activity independently of transcriptional changes (Cao et al., 2023). So, the absence of strong *ACACA* suppression under LCT/MCT does not necessarily imply that lipogenic flux is maintained but may instead indicate a shift toward post-translational regulation when MCFAs are present.

ACACB expression followed a similar pattern. While the most pronounced decreases occurred under LCT and IF, similar tendencies under CR and LCT/MCT suggest that *ACACB* expression is generally sensitive to both lipid availability and energy status. The functional relevance of its downregulation is supported by findings from *ACACB*-deficient mouse models, which show enhanced hepatic FAO and protection against hepatic steatosis under high-fat feeding (Abu-Elheiga et al., 2012). Although the complete deletion of *ACACB* represents an extreme case, these findings confirm that reducing ACC2-derived malonyl-CoA has a protective effect on hepatic lipid metabolism under lipid-oversupply conditions.

The expression of *FASN* further supports this anti-lipogenic adaptation. Its expression is tightly linked to carbohydrate availability and insulin signaling via SREBP-1c. *FASN* suppression under IF and KDs therefore reflects reduced insulin levels and negative feedback from incoming fatty acids (Moon et al., 2002; Nasser et al., 2022; Terry & Hay, 2024).

4.3 Tissue-Specific Regulation of Mitochondrial Fatty Acid Oxidation and Acetyl-CoA Handling

The following sections examine the different regulation of mitochondrial β-oxidation and acetyl-CoA handling, suggesting that lipid availability primarily drives hepatic oxidative capacity, whereas cardiac metabolism is more strongly shaped by energy status.

4.3.1 Heart

Cardiac expression of *ACADM* and *CRAT* was reduced under energy-restricted conditions, suggesting an adaptive transcriptional change of mitochondrial oxidative capacity in response to calorie limitation, consistent with a shift toward energy conservation.

In contrast to the findings by Nagao et al. (1993), who reported increased *ACADM* expression in rat hearts in response to high-fat feeding, the present study did not show such changes. The absence of upregulation under LCT and LCT/MCT feeding may reflect differences in species, diet composition or intervention duration, which highlights the context-dependent nature of cardiac metabolic adaptation. An alternative explanation is that, under LCT/MCT conditions, increased hepatic ketone body production may provide the heart preferred energy substrates, thereby reducing the transcriptional need to upregulate MCFA-specific oxidation pathways.

CRAT expression was significantly reduced under CR, consistent with a decreased need for acetyl-CoA buffering under conditions of limited substrate availability. Under lipid-rich conditions, an increased flux through β-oxidation would be expected to handle mitochondrial acetyl-CoA levels, potentially increasing the demand for *CRAT*-mediated buffering. While a slight increase in *CRAT* expression was observed under LCT feeding, this effect did not reach statistical significance. The lack of statistical significance suggests that cardiac *CRAT* regulation is relatively insensitive to dietary fat composition at the transcriptional level, potentially reflecting greater reliance on post-translational control.

4.3.2 Liver

In contrast to the heart, hepatic *ACADM* expression was significantly upregulated under both LCT and LCT/MCT feeding, indicating an increased transcriptional capacity for FAO in response to increased lipid supply. This is consistent with PPARα-mediated transcriptional activation under conditions of high fatty acid availability and reduced insulin signaling (Gulick et al., 1994; Rui, 2014).

The contrast to earlier findings by Nagao et al. (1993), who reported reduced hepatic *ACADM* under high-fat feeding, likely reflects the carbohydrate-restriction of the KDs used in the present study. This leads to decreased insulin and increased glucagon levels, which are known to promote hepatic FAO and may enhance transcription of genes such as *ACADM*. Thus, the combination of high lipid availability and a ketogenic hormonal environment may explain the observed upregulation. Under IF and CR, *ACADM* did not differ significantly from SD, suggesting that energy restriction per se does not further enhance hepatic FAO gene expression under these conditions.

CRAT expression was significantly lower under IF and CR compared to KDs, indicating an attenuation of acetyl-CoA handling under energy-restricted conditions. Under LCT feeding, a non-significant upward trend of *CRAT* was observed, consistent with an increased demand for acetyl-CoA buffering under conditions of enhanced β-oxidation. Overall, the hepatic data indicate that lipid availability in combination with ketogenic hormonal environment, is the primary driver of hepatic FAO gene expression, whereas *CRAT* appears to be more subtly regulated.

The divergence between *ACADM* regulation in liver and heart is one of the clearest findings in this data. The liver upregulates FAO capacity in response to lipid substrate supply, while the heart downregulates it under energy restriction. This reflects fundamentally different metabolic priorities in the two tissues.

4.4 Subtle Regulation of Mitochondrial Network Remodeling in Response to Diet

The following sections examine how key regulators of mitochondrial fusion and fission respond to dietary interventions in the heart and liver. While overall transcriptional changes were limited, subtle tissue-specific adaptations suggest that mitochondrial network remodeling is differentially regulated depending on energy status and substrate availability.

4.4.1 Heart

All genes involved in mitochondrial dynamics were expressed at markedly higher levels in cardiac than hepatic tissue, consistent with the heart's continuous dependence on mitochondrial function for contractile activity. The genes showed only minor transcriptional changes across dietary interventions, indicating that mitochondrial network integrity was largely preserved at the mRNA level.

The most notable exception was CR, which significantly reduced both *MFN1* and *MFN2*. This occurred alongside suppression of *ACADM* and *CRAT*, suggesting a broader coordinated downregulation of mitochondrial activity rather than a selective structural change. Whether the expression fall simply because less energy is needed under CR or whether this reflects an active structural adaptation of the mitochondrial network cannot be answered from mRNA data alone. The stability of *OPA1* and *FIS1* in parallel with reduced *MFN1/2* indicates a selective attenuation of OMM fusion without changes in inner membrane fusion or fission-related processes. This asymmetric pattern remains to be determined at the protein level.

Regarding *MFN2*, a prior analysis of the same tissue samples reported a significant downregulation under LCT (Sternberg et al., 2023), which was not observed in the present study. Importantly, this finding was based on protein quantification, whereas the present analysis measured mRNA expression. The absence of a transcriptional change therefore does not necessarily contradict Sternberg et al. (2023). Rather, these findings suggest that MFN2 regulation under LCT feeding may occur predominantly at the post-translational level.

The expression of *OPA1* and *FIS1* remained stable across all dietary conditions. This is consistent with the findings by Sternberg et al. (2023), who observed no significant changes in OPA1 expression under ketogenic conditions in cardiac tissue. This stability suggests that IMM fusion and fission processes are tightly preserved at the transcriptional level, even under metabolic stress.

4.4.2 Liver

In hepatic tissue, mitochondrial dynamics genes showed overall limited transcriptional variation, with mild diet-specific differences under IF and LCT/MCT conditions.

The expression of *MFN1* remained stable across all dietary groups. *MFN2* was significantly reduced under IF compared to SD and LCT/MCT. This suggests a mild

attenuation of mitochondrial fusion capacity under IF conditions. Although a previous study reported increased *MFN2* expression under prolonged CR (Rodríguez-López et al., 2020), this effect was not observed in the present study. The absence of such effects may reflect differences in intervention duration or metabolic context between the studies. Notably, *MFN2* expression under LCT/MCT was significantly higher compared to IF, suggesting that the two interventions drive the expression in opposing directions. This is consistent with previous findings by Newell et al. (2016), who reported upregulation of *MFN2* in hepatic tissue under ketogenic conditions. This may reflect an increased demand for mitochondrial-ER communication required for lipid handling (Zaman & Shutt, 2022). In contrast, its suppression during IF may reflect a shift toward mitochondrial fragmentation, potentially to facilitate mitophagy and maintain mitochondrial quality during sustained energy deprivation (Mann et al., 2024). Notably, mitochondrial fragmentation has been shown to reduce malonyl-CoA-mediated inhibition of CPT1, thereby increasing long-chain FAO capacity. This would be metabolically advantageous during fasting when lipid oxidation is the primary energy source (Ngo et al., 2023). The *MFN2* suppression observed under IF may therefore not only support mitochondrial quality control, but simultaneously enhance hepatic FAO capacity through CPT1 reactivation.

FIS1 expression was significantly higher under LCT/MCT compared to LCT, suggesting a mild regulation of mitochondrial fission-related transcription when both lipid classes are simultaneously fed. This could reflect an increased requirement for mitochondrial quality control under conditions of elevated and heterogenous lipid supply. While mitochondrial fission has been linked to enhanced long-chain FAO, these effects have primarily been attributed to Drp1-mediated mechanisms (Ngo et al., 2023). Given that *FIS1* functions as a regulatory adaptor whose precise role in mammalian fission remains debated, the functional significance of this transcriptional difference should be interpreted cautiously (Palmer et al., 2013).

Across all diets, *OPA1* expression remained stable relative to SD, consistent with previous findings under ketogenic conditions in hepatic tissue (Newell et al., 2016). Of note, studies using high-fat diets with substantial carbohydrate content have described reductions in OPA1 at the protein level (Zheng et al., 2023). This discrepancy may indicate that carbohydrate availability modulates mitochondrial dynamics but also suggests a possible post-translational regulation of OPA1.

4.5 Differential Regulation of Trp53 Expression in Response to Dietary Interventions

The following sections examine how dietary interventions influence *Trp53* expression in heart and liver. While energy restriction was associated with reduced transcriptional activity of *Trp53*, KDs showed only minor effects.

4.5.1 Heart

Under both IF and CR, the long *Trp53* isoform was significantly reduced relative to SD, whereas KDs did not induce significant changes. This suggests that energy restriction attenuates *Trp53*-mediated transcriptional activity in cardiac tissue, while increased lipid availability does not appear to trigger a comparable transcriptional response.

The short isoform showed no significant changes across dietary conditions compared to SD and remained expressed at low levels. This may indicate that its regulation is either post-translational or simply less metabolically responsive than the long isoform. Given their often context-dependent roles, subtle changes in short isoforms may not be captured at the mRNA level.

The stability of *Trp53* mRNA under ketogenic conditions does not necessarily stand in contrast to the findings by Wei et al. (2024), who reported increased p53 protein levels in cardiac tissue under ketogenic conditions. That study showed that KD-induced AMPK activation leads to caspase-2-mediated inhibition of Mouse Double Minute 2 (MDM2), a key negative regulator of p53. This resulted in protein stabilization and accumulation of p53 protein independent of transcriptional changes. In this context, the absence of increased *Trp53* mRNA expression in the present study suggests that p53 regulation under KDs may primarily occur at the post-translational level. Thus, transcriptional stability does not necessarily exclude enhanced p53 activity.

4.5.2 Liver

Hepatic *Trp53* expression showed a similar pattern to that observed in cardiac tissue. Energy-restricted conditions, particularly IF, were associated with significant reduction in the long isoform, while KDs were associated with stable or mildly elevated levels.

The downregulation of *Trp53* under IF is consistent with previous findings demonstrating that fasting-associated signaling pathways can suppress *Trp53* transcription. Activation

of FOXO1 under low insulin conditions has been shown to repress *Trp53* expression in hepatocytes (Oster et al., 2022).

The short isoform remained expressed at consistently low levels and did not show significant diet-dependent changes compared to SD. This further supports that the transcriptional regulation predominantly affects the long isoform. As in the heart, relatively stable *Trp53* expression under KDs do not exclude increased p53 protein activity. Post-translational stabilization via AMPK-MDM2 signaling under ketogenic conditions may be happening in the liver as well.

Taken together, the hepatic data indicate that *Trp53* expression is sensitive to energy restriction, likely mediated by insulin-FOXO1 signaling, whereas KDs do not strongly influence transcriptional regulation. Instead, p53 activity under ketogenic conditions may be governed by protein stabilization mechanisms.

5. Limitation

Despite providing insights into tissue-specific transcriptional adaptations to dietary interventions, several limitations of the present study should be considered when interpreting the findings.

First, the analysis was limited to mRNA expression. While this allows conclusions about transcriptional regulation, transcript levels do not necessarily reflect protein abundance or activity. This is particularly relevant for several pathways investigated in this study, including mitochondrial dynamics proteins such as MFN1/2 and OPA1, as well as p53 signaling, which are known to be strongly regulated at the post-translational level (Adaniya et al., 2019; Wei et al., 2024). As discussed in Section 4.4.1, the discrepancy between stable *MFN2* mRNA observed here and the reduced MFN2 protein reported by Sternberg et al. (2023) on the same tissue samples shows this point directly. Additional protein-level analyses such as Western blotting would be necessary to validate whether the transcriptional patterns observed here translate into functional differences.

Second, important upstream signaling pathways were not directly measured. Central metabolic regulators such as AMPK and PPARα play a major role in mediating the effects of energy restriction and altered lipid availability on mitochondrial function and gene expression. Without direct measurement of these pathways, for example the phosphorylation status of AMPK, the mechanistic interpretations remain partly inferential and only based on established literature rather than experimental confirmation within this study.

Third, RT-qPCR analysis from bulk tissue does not show cell-type specific contributions. Both the liver and heart consist of many different cell types (Malato et al., 2011; Pinto et al., 2016). Bulk tissue RNA sequencing captures averaged transcriptional signals across all cell types, meaning that cell-specific gene expression changes can be masked by stable expression in other cell types (Okada et al., 2022; Schaum et al., 2018; Tzec-Interián et al., 2025).

Future studies integrating transcript data with protein-level quantification will be important to more fully understand the mechanisms underlying diet-induced metabolic adaptations in heart and liver.

6. Conclusion

This study shows that dietary fat composition and energy availability differentially regulate metabolic gene expression in a tissue-specific manner. In particular, the comparison between LCT and LCT/MCT KDs highlights that not only lipid quantity, but also chain-length and metabolic pathway of fatty acids influence transcriptional regulation.

In the liver, KDs, particularly the LCT diet, were associated with an upregulation of genes involved in FAO and a suppression of lipogenic gene expression, consistent with a lipid-driven change toward increased oxidative metabolism. The attenuated transcriptional response under LCT/MCT suggests that the presence of rapidly oxidized MCFAs reduces the need for transcriptional reprogramming, possibly because their rapid hepatic oxidation limits intracellular lipid accumulation. IF reduced *MFN2*, *Trp53* and lipogenic gene expression, indicating that also energy availability is a modulator of metabolic gene programs.

In contrast, the heart showed only modest transcriptional changes across all dietary interventions. Under CR, a coordinated downregulation of *ACADM, CRAT, MFN1/2* and *Trp53* points to a broad shift toward energy conversation. Beyond this, dietary fat composition had limited impact on mRNA levels. This does not necessarily indicate a lack of metabolic adaptation. It rather reflects that cardiac metabolism may rely less on transcriptional regulation and more on rapid post-translational mechanisms to respond to nutritional changes. The post-translational stabilization of p53 via AMPK-MDM2 signaling under ketogenic conditions and the post-translational regulation of mitochondrial fusion proteins represent examples of such mechanisms. Transcriptional-level data alone therefore do not fully capture metabolic adaptation.

Overall, these findings show that transcriptional responses to a KD are not only shaped by carbohydrate restriction but by the specific fatty acid composition; and that how tissues respond to this differs fundamentally between the two organs. As with all murine dietary intervention studies, a direct translation to human physiology and settings is limited, especially given the highly controlled dietary conditions and practical challenges. Nevertheless, the present data provide a mechanistic insight into how distinct dietary lipid profiles differentially regulate gene expression in the liver and heart and highlights the need to consider both fatty acid structure and tissue context when evaluating the metabolic effects of KDs.

List of Abbreviations

ACACA	Acetyl-CoA carboxylase alpha
ACACB	Acetyl-CoA carboxylase beta
ACADM	Acyl-CoA dehydro-genase medium chain
ACC	Acetyl-CoA carboxylase
Acetyl-CoA	Acetyl-Coenzyme A
AMP	Adenosine mono-phosphate
AMPK	AMP-activated protein kinase
ATP	Adenosine triphosphate
BDH1	3-Hydroxybutyrate dehydrogenase
bp	Base pair
CACT	Carnitine-acylcarnitine translocase
cDNA	Complementary DNA
CPT	Carnitine palmitoyl-transferase
CR	Calorie restriction
CRAT	Carnitine acetyl-transferase
Ct	Cycle threshold
DNA	Deoxyribonucleic acid
DNL	De novo lipogenesis
Drp1	Dynamin-related protein 1
ER	Endoplasmic reticulum
eWAT	Epididymal white adipose tissue
FAO	Fatty acid oxidation
FASN	Fatty acid synthase
FIS1	Mitochondrial fission 1 protein
gDNA	Genomic DNA
GTPase	Guanosine triphosphatases
HKG	Housekeeping genes
IF	Intermittent fasting
IMM	Inner mitochondrial membrane
HMGCL	3-Hydroxy-3-methyl-glutaryl-CoA lyase
HMGCS2	3-Hydroxy-3-methyl-glutaryl-CoA synthase
KD	Ketogenic diet
LCFA	Long-chain fatty acids
LCT	Long-chain triglyceride
Malonyl-CoA	Malonyl-Coenzyme A
MCAD	Medium-chain acyl-CoA dehydrogenase
MCT	Medium-chain triglyceride
MCFA	Medium-chain fatty acid
MDM2	Mouse double minute 2
MFN1	Mitofusin 1
MFN2	Mitofusin 2
mRNA	Messenger ribonucleic acid
OMM	Outer mitochondrial membrane
OPA1	Optic atrophy 1
PDH	Pyruvate dehydrogenase complex

PUFA	Polyunsaturated fatty acid
qPCR	Quantitative polymerase chain reaction
RNA	Ribonucleic acid
Rpl4	Ribosomal protein L4
RT-qPCR	Real-time quantitative PCR
TBP	TATA box binding protein
TCA Cycle	Tricarboxylic acid cycle
SCOT	Succinyl-CoA:3-oxoacid-CoA transferase
SCREBP-1c	Sterol regulatory element-binding protein 1c
SD	Standard diet
β-OHB	β-Hydroxybutyrate

Literature

Abu-Elheiga, L., Wu, H., Gu, Z., Bressler, R., & Wakil, S. J. (2012). Acetyl-CoA Carboxylase 2−/− Mutant Mice are Protected against Fatty Liver under High-fat, High-carbohydrate Dietary and de Novo Lipogenic Conditions. *Journal of Biological Chemistry*, *287*(15), 12578–12588. https://doi.org/10.1074/jbc.M111.309559

Adaniya, S. M., O-Uchi, J., Cypress, M. W., Kusakari, Y., & Jhun, B. S. (2019). Posttranslational modifications of mitochondrial fission and fusion proteins in cardiac physiology and pathophysiology. *American journal of physiology. Cell physiology*, *316*(5), C583–C604. https://doi.org/10.1152/ajpcell.00523.2018

Almog, N., Goldfinger, N., & Rotter, V. (2000). p53-dependent apoptosis is regulated by a C-terminally alternatively spliced form of murine p53. *Oncogene*, *19*(30), 3395–3403. https://doi.org/10.1038/sj.onc.1203673

Altamimi, T. R., Thomas, P. D., Darwesh, A. M., Fillmore, N., Mahmoud, M. U., Zhang, L., Gupta, A., Al Batran, R., Seubert, J. M., & Lopaschuk, G. D. (2018). Cytosolic carnitine acetyltransferase as a source of cytosolic acetyl-CoA: A possible mechanism for regulation of cardiac energy metabolism. *Biochemical Journal*, *475*(5), 959–976. https://doi.org/10.1042/BCJ20170823

Anekwe, C., Chandrasekaran, P., & Stanford, F. C. (2020). Ketogenic Diet-induced Elevated Cholesterol, Elevated Liver Enzymes and Potential Non-alcoholic Fatty Liver Disease. *Cureus*. https://doi.org/10.7759/cureus.6605

Bach, A. C., Frey, A., & Lutz, O. (1989). Clinical and experimental effects of medium-chain-triglyceride-based fat Emulsions—A review. *Clinical Nutrition*, *8*(5), 223–235. https://doi.org/10.1016/0261-5614(89)90032-0

Berndt, J., Kovacs, P., Ruschke, K., Klöting, N., Fasshauer, M., Schön, M. R., Körner, A., Stumvoll, M., & Blüher, M. (2007). Fatty acid synthase gene expression in human adipose tissue: Association with obesity and type 2 diabetes. *Diabetologia*, *50*(7), 1472–1480. https://doi.org/10.1007/s00125-007-0689-x

Bhavsar, N., & St-Onge, M.-P. (2016). The diverse nature of saturated fats and the case of medium-chain triglycerides: How one recommendation may not fit all. *Current Opinion in Clinical Nutrition and Metabolic Care*, *19*(2), 81–87. https://doi.org/10.1097/MCO.0000000000000249

Boone, C., & Lewis, S. C. (2024). Bridging lipid metabolism and mitochondrial genome maintenance. *Journal of Biological Chemistry*, *300*(8), 107498. https://doi.org/10.1016/j.jbc.2024.107498

Brattelid, T., Winer, L. H., Levy, F. O., Liestøl, K., Sejersted, O. M., & Andersson, K. B. (2010). Reference gene alternatives to Gapdh in rodent and human heart failure gene expression studies. *BMC Molecular Biology*, *11*(1). https://doi.org/10.1186/1471-2199-11-22

Bueno, N. B., de Melo, I. V., Florêncio, T. T., & Sawaya, A. L. (2015). Dietary medium-chain triacylglycerols versus long-chain triacylglycerols for body composition in adults: systematic review and meta-analysis of randomized controlled trials. *Journal of the American College of Nutrition*, *34*(2), 175–183. https://doi.org/10.1080/07315724.2013.879844

Burke, N., Hall, A., & Hausenloy, D. (2015). OPA1 in Cardiovascular Health and Disease. *Current Drug Targets*, *16*(8), 912–920. https://doi.org/10.2174/1389450116666150102113648

Calhoon, E. A., Ro, J., & Williams, J. B. (2015). Perspectives on the membrane fatty acid unsaturation/pacemaker hypotheses of metabolism and aging. *Chemistry and Physics of Lipids*, *191*, 48–60. https://doi.org/10.1016/j.chemphyslip.2015.08.008

Cao, H., Cai, Q., Guo, W., Su, Q., Qin, H., Wang, T., Xian, Y., Zeng, L., Cai, M., Guan, H., Chen, S., Liang, H., & Xu, F. (2023). Malonylation of Acetyl-CoA carboxylase 1 promotes hepatic steatosis and is attenuated by ketogenic diet in NAFLD. *Cell Reports*, *42*(4), 112319. https://doi.org/10.1016/j.celrep.2023.112319

Chandhok, G., Lazarou, M., & Neumann, B. (2018). Structure, function, and regulation of mitofusin-2 in health and disease. *Biological Reviews*, *93*(2), 933–949. https://doi.org/10.1111/brv.12378

Chen, H., Chomyn, A., & Chan, D. C. (2005). Disruption of Fusion Results in Mitochondrial Heterogeneity and Dysfunction. *Journal of Biological Chemistry*, *280*(28), 26185–26192. https://doi.org/10.1074/jbc.M503062200

D C. Harvey, C. J., Schofield, G. M., Williden, M., & McQuillan, J. A. (2018). The Effect of Medium Chain Triglycerides on Time to Nutritional Ketosis and Symptoms of Keto-Induction in Healthy Adults: A Randomised Controlled Clinical Trial. *Journal of Nutrition and Metabolism*, *2018*, 1–9. https://doi.org/10.1155/2018/2630565

Da Dalt, L., Cabodevilla, A. G., Goldberg, I. J., & Norata, G. D. (2023). Cardiac lipid metabolism, mitochondrial function, and heart failure. *Cardiovascular Research*, *119*(10), 1905–1914. https://doi.org/10.1093/cvr/cvad100

Dai, W., & Jiang, L. (2019). Dysregulated Mitochondrial Dynamics and Metabolism in Obesity, Diabetes, and Cancer. *Frontiers in Endocrinology*, *10*, 570. https://doi.org/10.3389/fendo.2019.00570

Dambrova, M., Makrecka-Kuka, M., Kuka, J., Vilskersts, R., Nordberg, D., Attwood, M. M., Smesny, S., Sen, Z. D., Guo, A. C., Oler, E., Tian, S., Zheng, J., Wishart, D. S., Liepinsh, E., & Schiöth, H. B. (2022). Acylcarnitines: Nomenclature, Biomarkers, Therapeutic Potential, Drug Targets, and Clinical Trials. *Pharmacological Reviews*, *74*(3), 506–551. https://doi.org/10.1124/pharmrev.121.000408

Day, P. E. L., Chambers, K. F., Winterbone, M. S., García-Blanco, T., Vauzour, D., & Kroon, P. A. (2018). Validation of control genes and a standardised protocol for quantifying gene expression in the livers of C57BL/6 and ApoE−/− mice. *Scientific Reports*, *8*(1). https://doi.org/10.1038/s41598-018-26431-3

De Jonge, H. J. M., Fehrmann, R. S. N., De Bont, E. S. J. M., Hofstra, R. M. W., Gerbens, F., Kamps, W. A., De Vries, E. G. E., Van Der Zee, A. G. J., Te Meerman, G. J., & Ter Elst, A. (2007). Evidence Based Selection of Housekeeping Genes. *PLoS ONE*, *2*(9), e898. https://doi.org/10.1371/journal.pone.0000898

Dikalov, S., Panov, A., & Dikalova, A. (2024). Critical Role of Mitochondrial Fatty Acid Metabolism in Normal Cell Function and Pathological Conditions. *International Journal of Molecular Sciences*, *25*(12), 6498. https://doi.org/10.3390/ijms25126498

Dong, J., Li, M., Peng, R., Zhang, Y., Qiao, Z., & Sun, N. (2024). ACACA reduces lipid accumulation through dual regulation of lipid metabolism and mitochondrial function via AMPK- PPARα- CPT1A axis. *Journal of Translational Medicine*, *22*(1), 196. https://doi.org/10.1186/s12967-024-04942-0

Dunn, E., Zhang, B., Sahota, V. K., & Augustin, H. (2023). Potential benefits of medium chain fatty acids in aging and neurodegenerative disease. *Frontiers in Aging Neuroscience*, *15*, 1230467. https://doi.org/10.3389/fnagi.2023.1230467

Emanuele, F., Biondo, M., Tomasello, L., Arnaldi, G., & Guarnotta, V. (2025). Ketogenic Diet in Steatotic Liver Disease: A Metabolic Approach to Hepatic Health. *Nutrients*, *17*(7), 1269. https://doi.org/10.3390/nu17071269

Engin, A. (2017). The Definition and Prevalence of Obesity and Metabolic Syndrome. In A. B. Engin & A. Engin (Hrsg.), *Obesity and Lipotoxicity* (Bd. 960, S. 1–17). Springer International Publishing. https://doi.org/10.1007/978-3-319-48382-5_1

Frohman, M. A. (2015). Role of mitochondrial lipids in guiding fission and fusion. *Journal of Molecular Medicine*, *93*(3), 263–269. https://doi.org/10.1007/s00109-014-1237-z

Galic, S., Loh, K., Murray-Segal, L., Steinberg, G. R., Andrews, Z. B., & Kemp, B. E. (2018). AMPK signaling to acetyl-CoA carboxylase is required for fasting- and cold-induced appetite but not thermogenesis. *eLife*, *7*, e32656. https://doi.org/10.7554/eLife.32656

Gomes, L. C., & Scorrano, L. (2008). High levels of Fis1, a pro-fission mitochondrial protein, trigger autophagy. *Biochimica et Biophysica Acta (BBA) - Bioenergetics*, *1777*(7–8), 860–866. https://doi.org/10.1016/j.bbabio.2008.05.442

Gregor, A., Huber, L., Auernigg-Haselmaier, S., Sternberg, F., Billerhart, M., Dunkel, A., Somoza, V., Ogris, M., Kofler, B., Longo, V. D., König, J., & Duszka, K.

(2022). A Comparison of the Impact of Restrictive Diets on the Gastrointestinal Tract of Mice. *Nutrients*, *14*(15), 3120. https://doi.org/10.3390/nu14153120

Gulick, T., Cresci, S., Caira, T., Moore, D. D., & Kelly, D. P. (1994). The peroxisome proliferator-activated receptor regulates mitochondrial fatty acid oxidative enzyme gene expression. *Proceedings of the National Academy of Sciences*, *91*(23), 11012–11016. https://doi.org/10.1073/pnas.91.23.11012

Hailu, K. T., Salib, K., Savithri Nandeesha, S., Kasagga, A., Hawrami, C., Ricci, E., & Hamid, P. (2024). The Effect of Fasting on Cardiovascular Diseases: A Systematic Review. *Cureus*. https://doi.org/10.7759/cureus.53221

Halliwell, B., & Chirico, S. (1993). Lipid peroxidation: Its mechanism, measurement, and significance. *The American Journal of Clinical Nutrition*, *57*(5), 715S-725S. https://doi.org/10.1093/ajcn/57.5.715S

Han, Y., Liu, Y., Zhen, J., Hou, S., Zhang, B., Cui, Z., Wan, Q., & Feng, H. (2022). P53 regulates mitochondrial biogenesis via transcriptionally induction of mitochondrial ribosomal protein L12. *Experimental Cell Research*, *418*(1), 113249. https://doi.org/10.1016/j.yexcr.2022.113249

Harada, N., Oda, Z., Hara, Y., Fujinami, K., Okawa, M., Ohbuchi, K., Yonemoto, M., Ikeda, Y., Ohwaki, K., Aragane, K., Tamai, Y., & Kusunoki, J. (2007). Hepatic De Novo Lipogenesis Is Present in Liver-Specific ACC1-Deficient Mice. *Molecular and Cellular Biology*, *27*(5), 1881–1888. https://doi.org/10.1128/MCB.01122-06

He, K., Wei, D., Liu, Q., Liu, X., Zhou, D., Chen, S., Zhu, D., & Xu, X. (2024). Identification of stable housekeeping genes in mouse liver for studying carbon tetrachloride-induced injury and cellular senescence. *Scientific Reports*, *14*(1), 26544. https://doi.org/10.1038/s41598-024-78183-y

He, T., Sha, J., Hu, Y., Shao, C., Zhou, Y., Chen, L., Yao, J., & Gao, J. (2025). *Single-Cell Sequencing Identifies the Crucial Role of Mitochondrial Fission-Fusion Balance in Cardiac Hypertrophy Progression*. Bioinformatics. https://doi.org/10.1101/2025.02.13.638057

Hecker, M., Sommer, N., Voigtmann, H., Pak, O., Mohr, A., Wolf, M., Vadász, I., Herold, S., Weissmann, N., Morty, R. E., Seeger, W., & Mayer, K. (2014). Impact of Short- and Medium-Chain Fatty Acids on Mitochondrial Function in Severe Inflammation. *Journal of Parenteral and Enteral Nutrition*, *38*(5), 587–594. https://doi.org/10.1177/0148607113489833

Hernández Borrero, L. J., & El-Deiry, W. S. (2021). Tumor suppressor p53: Biology, signaling pathways, and therapeutic targeting. *Biochimica et Biophysica Acta (BBA) - Reviews on Cancer*, *1876*(1), 188556. https://doi.org/10.1016/j.bbcan.2021.188556

Hilary, S., Östlundh, L., Platat, C., Al-Rifai, R. H., Almehairbi, O., Alshamsi, F., Ali, H. I., Al Dhaheri, A. S., Cheikh Ismail, L., & Stojanovska, L. (2024). Effect of

ketogenic diets on lipid metabolism in adults: Protocol for a systematic review. *BMJ Open*, *14*(9), e076938. https://doi.org/10.1136/bmjopen-2023-076938

Huang, T.-Y., Goldsmith, F. R., Fuller, S. E., Simon, J., Batdorf, H. M., Scott, M. C., Essajee, N. M., Brown, J. M., Burk, D. H., Morrison, C. D., Burke, S. J., Collier, J. J., & Noland, R. C. (2020). Response of Liver Metabolic Pathways to Ketogenic Diet and Exercise Are Not Additive. *Medicine & Science in Sports & Exercise*, *52*(1), 37–48. https://doi.org/10.1249/MSS.0000000000002105

Ihenacho, U. K., Meacham, K. A., Harwig, M. C., Widlansky, M. E., & Hill, R. B. (2021). Mitochondrial Fission Protein 1: Emerging Roles in Organellar Form and Function in Health and Disease. *Frontiers in Endocrinology*, *12*, 660095. https://doi.org/10.3389/fendo.2021.660095

Jadhav, H. B., & Annapure, U. S. (2023). Triglycerides of medium-chain fatty acids: A concise review. *Journal of Food Science and Technology*, *60*(8), 2143–2152. https://doi.org/10.1007/s13197-022-05499-w

Jandacek, R. J. (1994). *Food Components to Enhance Performance: An Evaluation of Potential Performance-Enhancing Food Components for Operational Rations* (S. 4563). National Academies Press. https://doi.org/10.17226/4563

Javadov, S., Rajapurohitam, V., Kilić, A., Hunter, J. C., Zeidan, A., Said Faruq, N., Escobales, N., & Karmazyn, M. (2011). Expression of mitochondrial fusion–fission proteins during post-infarction remodeling: The effect of NHE-1 inhibition. *Basic Research in Cardiology*, *106*(1), 99–109. https://doi.org/10.1007/s00395-010-0122-3

Jensen-Urstad, A. P. L., & Semenkovich, C. F. (2012). Fatty acid synthase and liver triglyceride metabolism: Housekeeper or messenger? *Biochimica et Biophysica Acta (BBA) - Molecular and Cell Biology of Lipids*, *1821*(5), 747–753. https://doi.org/10.1016/j.bbalip.2011.09.017

Joruiz, S. M., & Bourdon, J. C. (2016). p53 Isoforms: Key Regulators of the Cell Fate Decision. *Cold Spring Harbor perspectives in medicine*, *6*(8), a026039. https://doi.org/10.1101/cshperspect.a026039

Katz, S., Lechel, A., Obenauf, A. C., Begus–Nahrmann, Y., Kraus, J. M., Hoffmann, E. M., Duda, J., Eshraghi, P., Hartmann, D., Liss, B., Schirmacher, P., Kestler, H. A., Speicher, M. R., & Rudolph, K. L. (2012). Disruption of Trp53 in Livers of Mice Induces Formation of Carcinomas With Bilineal Differentiation. *Gastroenterology*, *142*(5), 1229-1239.e3. https://doi.org/10.1053/j.gastro.2012.02.009

Kennedy, A. R., Pissios, P., Otu, H., Xue, B., Asakura, K., Furukawa, N., Marino, F. E., Liu, F.-F., Kahn, B. B., Libermann, T. A., & Maratos-Flier, E. (2007). A high-fat, ketogenic diet induces a unique metabolic state in mice. *American Journal of*

Physiology-Endocrinology and Metabolism, *292*(6), E1724–E1739. https://doi.org/10.1152/ajpendo.00717.2006

Kersten S. (2014). Integrated physiology and systems biology of PPARα. *Molecular metabolism*, *3*(4), 354–371. https://doi.org/10.1016/j.molmet.2014.02.002

Kim, J. J., Wang, M., & Paschke, R. (1993). Crystal structures of medium-chain acyl-CoA dehydrogenase from pig liver mitochondria with and without substrate. *Proceedings of the National Academy of Sciences*, *90*(16), 7523–7527. https://doi.org/10.1073/pnas.90.16.7523

Kim, K.-H. (1997). Regulation of Mammalian Acetyl-Coenzyme A Carboxylase. *Annual Review of Nutrition*, *17*(1), 77–99. https://doi.org/10.1146/annurev.nutr.17.1.77

Kolb, H., Kempf, K., Röhling, M., Lenzen-Schulte, M., Schloot, N. C., & Martin, S. (2021). Ketone bodies: From enemy to friend and guardian angel. *BMC Medicine*, *19*(1), 313. https://doi.org/10.1186/s12916-021-02185-0

Koltai, T., Reshkin, S. J., Baltazar, F., & Fliegel, L. (2021). Lipid metabolism part I. In *Prostate Cancer Metabolism* (S. 71–135). Elsevier. https://doi.org/10.1016/B978-0-323-90528-2.00013-8

Kyriazis, I., Vassi, E., Alvanou, M., Angelakis, C., Skaperda, Z., Tekos, F., Garikipati, V., Spandidos, D., & Kouretas, D. (2022). The impact of diet upon mitochondrial physiology (Review). *International Journal of Molecular Medicine*, *50*(5), 135. https://doi.org/10.3892/ijmm.2022.5191

Labarthe, F., Gélinas, R., & Des Rosiers, C. (2008). Medium-chain Fatty Acids as Metabolic Therapy in Cardiac Disease. *Cardiovascular Drugs and Therapy*, *22*(2), 97–106. https://doi.org/10.1007/s10557-008-6084-0

Lee, H., Lee, T. J., Galloway, C. A., Zhi, W., Xiao, W., De Mesy Bentley, K. L., Sharma, A., Teng, Y., Sesaki, H., & Yoon, Y. (2023). The mitochondrial fusion protein OPA1 is dispensable in the liver and its absence induces mitohormesis to protect liver from drug-induced injury. *Nature Communications*, *14*(1), 6721. https://doi.org/10.1038/s41467-023-42564-0

Lee, Y., Jeong, S.-Y., Karbowski, M., Smith, C. L., & Youle, R. J. (2004). Roles of the Mammalian Mitochondrial Fission and Fusion Mediators Fis1, Drp1, and Opa1 in Apoptosis. *Molecular Biology of the Cell*, *15*(11), 5001–5011. https://doi.org/10.1091/mbc.e04-04-0294

Lee, Y. T., Senturk, M., Guan, Y., & Wang, M. C. (2024). Bacteria-organelle communication in physiology and disease. *The Journal of cell biology*, *223*(7), e202310134. https://doi.org/10.1083/jcb.202310134

Li, L., Martin-Levilain, J., Jiménez-Sánchez, C., Karaca, M., Foti, M., Martinou, J.-C., & Maechler, P. (2019). In vivo stabilization of OPA1 in hepatocytes potentiates mitochondrial respiration and gluconeogenesis in a prohibitin-dependent way.

Journal of Biological Chemistry, *294*(34), 12581–12598. https://doi.org/10.1074/jbc.RA119.007601

Li, X., & Bi, X. (2023). Integrated Control of Fatty Acid Metabolism in Heart Failure. *Metabolites*, *13*(5), 615. https://doi.org/10.3390/metabo13050615

Li, Y., Liang, J., Tian, X., Chen, Q., Zhu, L., Wang, H., Liu, Z., Dai, X., Bian, C., & Sun, C. (2023). Intermittent fasting promotes adipocyte mitochondrial fusion through Sirt3-mediated deacetylation of Mdh2. *British Journal of Nutrition*, *130*(9), 1473–1486. https://doi.org/10.1017/S000711452300048X

Lim, S. C., Tajika, M., Shimura, M., Carey, K. T., Stroud, D. A., Murayama, K., Ohtake, A., & McKenzie, M. (2018). Loss of the Mitochondrial Fatty Acid β-Oxidation Protein Medium-Chain Acyl-Coenzyme A Dehydrogenase Disrupts Oxidative Phosphorylation Protein Complex Stability and Function. *Scientific Reports*, *8*(1), 153. https://doi.org/10.1038/s41598-017-18530-4

Liou, Y.-H., Personnaz, J., Jacobi, D., Knudsen, N. H., Chalom, M. M., Starost, K. A., Nnah, I. C., & Lee, C.-H. (2022). Hepatic Fis1 regulates mitochondrial integrated stress response and improves metabolic homeostasis. *JCI Insight*, *7*(4), e150041. https://doi.org/10.1172/jci.insight.150041

Longnus, S. L., Wambolt, R. B., Barr, R. L., Lopaschuk, G. D., & Allard, M. F. (2001). Regulation of myocardial fatty acid oxidation by substrate supply. *American Journal of Physiology-Heart and Circulatory Physiology*, *281*(4), H1561–H1567. https://doi.org/10.1152/ajpheart.2001.281.4.H1561

Longo, R., Peri, C., Cricrì, D., Coppi, L., Caruso, D., Mitro, N., De Fabiani, E., & Crestani, M. (2019). Ketogenic Diet: A New Light Shining on Old but Gold Biochemistry. *Nutrients*, *11*(10), 2497. https://doi.org/10.3390/nu11102497

Madeira, C. A., Anselmo, C., Costa, J. M., Bonito, C. A., Ferreira, R. J., Santos, D. J. V. A., Wanders, R. J., Vicente, J. B., Ventura, F. V., & Leandro, P. (2023). Functional and structural impact of 10 ACADM missense mutations on human medium chain acyl-Coa dehydrogenase. *Biochimica et Biophysica Acta (BBA) - Molecular Basis of Disease*, *1869*(7), https://doi.org/10.1016/j.bbadis.2023.166766

Mak, T. W., Hauck, L., Grothe, D., & Billia, F. (2017). P53 regulates the cardiac transcriptome. *Proceedings of the National Academy of Sciences*, *114*(9), 2331–2336. https://doi.org/10.1073/pnas.1621436114

Malato, Y., Naqvi, S., Schürmann, N., Ng, R., Wang, B., Zape, J., Kay, M. A., Grimm, D., & Willenbring, H. (2011). Fate tracing of mature hepatocytes in mouse liver homeostasis and regeneration. *The Journal of clinical investigation*, *121*(12), 4850–4860. https://doi.org/10.1172/JCI59261

Mann, J. P., Tábara, L. C., Patel, S., Pushpa, P., Alvarez-Guaita, A., Dong, L., Haider, A., Lim, K., Tandon, P., Scurria, F., Minchin, J. E. N., O'Rahilly S., S., Fazakerley, D. J., Prudent, J., Semple, R. K., & Savage, D. B. (2024). Loss of

Mfn1 but not Mfn2 enhances adipogenesis. *PLOS ONE*, *19*(12), e0306243. https://doi.org/10.1371/journal.pone.0306243

Marcel, V., Dichtel-Danjoy, M. L., Sagne, C., Hafsi, H., Ma, D., Ortiz-Cuaran, S., Olivier, M., Hall, J., Mollereau, B., Hainaut, P., & Bourdon, J. C. (2011). Biological functions of p53 isoforms through evolution: lessons from animal and cellular models. *Cell death and differentiation*, *18*(12), 1815–1824. https://doi.org/10.1038/cdd.2011.120

Marcondes-de-Castro, I. A., Reis-Barbosa, P. H., Marinho, T. S., Aguila, M. B., & Mandarim-de-Lacerda, C. A. (2023). AMPK/mTOR pathway significance in healthy liver and non-alcoholic fatty liver disease and its progression. *Journal of gastroenterology and hepatology*, *38*(11), 1868–1876. https://doi.org/10.1111/jgh.16272

Matyi, S., Jackson, J., Garrett, K., Deepa, S. S., & Unnikrishnan, A. (2018). The effect of different levels of dietary restriction on glucose homeostasis and metabolic memory. *GeroScience*, *40*(2), 139–149. https://doi.org/10.1007/s11357-018-0011-5

Mayr, J. A. (2015). Lipid metabolism in mitochondrial membranes. *Journal of Inherited Metabolic Disease*, *38*(1), 137–144. https://doi.org/10.1007/s10545-014-9748-x

Meade, R., Ibrahim, D., Engel, C., Belaygorod, L., Arif, B., Hsu, F.-F., Adak, S., Catlett, R., Zhou, M., Ilagan, Ma. X. G., Semenkovich, C. F., & Zayed, M. A. (2025). Targeting fatty acid synthase reduces aortic atherosclerosis and inflammation. *Communications Biology*, *8*(1), 262. https://doi.org/10.1038/s42003-025-07656-1

Men, H., Cai, H., Cheng, Q., Zhou, W., Wang, X., Huang, S., Zheng, Y., & Cai, L. (2021). The regulatory roles of p53 in cardiovascular health and disease. *Cellular and Molecular Life Sciences*, *78*(5), 2001–2018. https://doi.org/10.1007/s00018-020-03694-6

Merritt, A. M., & Julliand, V. (2013). Gastrointestinal physiology. In *Equine Applied and Clinical Nutrition* (S. 3–32). Elsevier. https://doi.org/10.1016/B978-0-7020-3422-0.00001-8

Milder, J., & Patel, M. (2012). Modulation of oxidative stress and mitochondrial function by the ketogenic diet. *Epilepsy Research*, *100*(3), 295–303. https://doi.org/10.1016/j.eplepsyres.2011.09.021

Mishra, P., & Chan, D. C. (2016). Metabolic regulation of mitochondrial dynamics. *Journal of Cell Biology*, *212*(4), 379–387. https://doi.org/10.1083/jcb.201511036

Mooli, R. G. R., & Ramakrishnan, S. K. (2022). Emerging Role of Hepatic Ketogenesis in Fatty Liver Disease. *Frontiers in Physiology*, *13*, 946474. https://doi.org/10.3389/fphys.2022.946474

Moon, Y. S., Latasa, M.-J., Griffin, M. J., & Sul, H. S. (2002). Suppression of fatty acid synthase promoter by polyunsaturated fatty acids. *Journal of Lipid Research*, *43*(5), 691–698. https://doi.org/10.1016/S0022-2275(20)30110-3

Nagao, M., Parimoo, B., & Tanaka, K. (1993). Developmental, nutritional, and hormonal regulation of tissue-specific expression of the genes encoding various acyl-CoA dehydrogenases and alpha-subunit of electron transfer flavoprotein in rat. *Journal of Biological Chemistry*, *268*(32), 24114–24124. https://doi.org/10.1016/S0021-9258(20)80500-6

Nasser, S., Solé, T., Vega, N., Thomas, T., Balcerczyk, A., Strigini, M., & Pirola, L. (2022). Ketogenic diet administration to mice after a high-fat-diet regimen promotes weight loss, glycemic normalization and induces adaptations of ketogenic pathways in liver and kidney. *Molecular Metabolism*, *65*, 101578. https://doi.org/10.1016/j.molmet.2022.101578

National Center for Biotechnology Information. (2025, Februar 25). National Library of Medicine. *Primer Blast*. https://www.ncbi.nlm.nih.gov/tools/primer-blast/

National Center for Biotechnology Information (2026) Newell, C., Shutt, T. E., Ahn, Y., Hittel, Dustin. S., Khan, A., Rho, J. M., & Shearer, J. (2016). Tissue Specific Impacts of a Ketogenic Diet on Mitochondrial Dynamics in the BTBRT+tf/j Mouse. *Frontiers in Physiology*, *7*. https://doi.org/10.3389/fphys.2016.00654

Ngo, J., Choi, D. W., Stanley, I. A., Stiles, L., Molina, A. J. A., Chen, P., Lako, A., Sung, I. C. H., Goswami, R., Kim, M., Miller, N., Baghdasarian, S., Kim-Vasquez, D., Jones, A. E., Roach, B., Gutierrez, V., Erion, K., Divakaruni, A. S., Liesa, M., … Shirihai, O. S. (2023). Mitochondrial morphology controls fatty acid utilization by changing CPT1 sensitivity to malonyl-CoA. *The EMBO Journal*, *42*(11), e111901. https://doi.org/10.15252/embj.2022111901

Nguyen, B. Y., Ruiz-Velasco, A., Bui, T., Collins, L., Wang, X., & Liu, W. (2019). Mitochondrial function in the heart: The insight into mechanisms and therapeutic potentials. *British Journal of Pharmacology*, *176*(22), 4302–4318. https://doi.org/10.1111/bph.14431

Nguyen, P., Leray, V., Diez, M., Serisier, S., Bloc'h, J. L., Siliart, B., & Dumon, H. (2008). Liver lipid metabolism. *Journal of Animal Physiology and Animal Nutrition*, *92*(3), 272–283. https://doi.org/10.1111/j.1439-0396.2007.00752.x

Nolfi-Donegan, D., Braganza, A., & Shiva, S. (2020). Mitochondrial electron transport chain: Oxidative phosphorylation, oxidant production, and methods of measurement. *Redox Biology*, *37*, 101674. https://doi.org/10.1016/j.redox.2020.101674

Okada, D., Zheng, C., & Cheng, J. H. (2022). Mathematical model for the relationship between single-cell and bulk gene expression to clarify the interpretation of bulk gene expression data. *Computational and structural biotechnology journal*, *20*, 4850–4859. https://doi.org/10.1016/j.csbj.2022.08.062

Okuda, T., & Morita, N. (2012). A very low carbohydrate ketogenic diet prevents the progression of hepatic steatosis caused by hyperglycemia in a juvenile obese mouse model. *Nutrition & Diabetes*, *2*(11), e50–e50. https://doi.org/10.1038/nutd.2012.24

Origene Technologies. (2025a, Februar 26). Origene Technologies. *MFN1 (mouse) qPCR primer pair (NM_024200)*. https://www.origene.com/catalog/gene-expression/qpcr-primer-pairs/mp208303-mfn1-mouse-qpcr-primer-pair-nm-024200

Origene Technologies. (2025b, Februar 26). Origene Technologies. *FIS1 (mouse) qPCR primer pair (NM_025562)*. https://www.origene.com/catalog/gene-expression/qpcr-primer-pairs/mp204868-fis1-mouse-qpcr-primer-pair-nm-025562

Oster, M., Galhuber, M., Krstic, J., Steinhoff, J. S., Lenihan-Geels, G., Wulff, S., Kiefer, M. F., Petricek, K. M., Wowro, S. J., Flores, R. E., Yang, N., Li, C., Meng, Y., Reinisch, I., Sommerfeld, M., Weger, S., Habisch, H., Madl, T., Schulz, T. J., …Schupp, M. (2022). Hepatic p53 is regulated by transcription factor FOXO1 and acutely controls glycogen homeostasis. *Journal of Biological Chemistry*, *298*(9), 102287. https://doi.org/10.1016/j.jbc.2022.102287

Palmer, C. S., Elgass, K. D., Parton, R. G., Osellame, L. D., Stojanovski, D., & Ryan, M. T. (2013). Adaptor proteins MiD49 and MiD51 can act independently of Mff and Fis1 in Drp1 recruitment and are specific for mitochondrial fission. *The Journal of biological chemistry*, *288*(38), 27584–27593. https://doi.org/10.1074/jbc.M113.479873

Paoli, A., Bianco, A., Moro, T., Mota, J. F., & Coelho-Ravagnani, C. D. F. (2023). The Effects of Ketogenic Diet on Insulin Sensitivity and Weight Loss, Which Came First: The Chicken or the Egg? *Nutrients*, *15*(14), 3120. https://doi.org/10.3390/nu15143120

Papamandjaris, A., MacDougall, D. E., & Jones, P. J. (1998). Medium chain fatty acid metabolism and energy expenditure: Obesity treatment implications. *Life sciences*, *62*(14), 1203–1215. https://doi.org/10.1016/s0024-3205(97)01143-0

Pascual, F., & Coleman, R. A. (2016). Fuel availability and fate in cardiac metabolism: A tale of two substrates. *Biochimica et Biophysica Acta (BBA) - Molecular and Cell Biology of Lipids*, *1861*(10), 1425–1433. https://doi.org/10.1016/j.bbalip.2016.03.014

Peng, K.-Y., Watt, M. J., Rensen, S., Greve, J. W., Huynh, K., Jayawardana, K. S., Meikle, P. J., & Meex, R. C. R. (2018). Mitochondrial dysfunction-related lipid changes occur in nonalcoholic fatty liver disease progression. *Journal of Lipid Research*, *59*(10), 1977–1986. https://doi.org/10.1194/jlr.M085613

Pereyra, A. S., McLaughlin, K. L., Buddo, K. A., & Ellis, J. M. (2023). Medium-chain fatty acid oxidation is independent of L -carnitine in liver and kidney but not in heart and skeletal muscle. *American Journal of Physiology-Gastrointestinal and Liver Physiology*, *325*(4), G287–G294. https://doi.org/10.1152/ajpgi.00105.2023

Pinto, A. R., Ilinykh, A., Ivey, M. J., Kuwabara, J. T., D'Antoni, M. L., Debuque, R., Chandran, A., Wang, L., Arora, K., Rosenthal, N. A., & Tallquist, M. D. (2016). Revisiting Cardiac Cellular Composition. *Circulation research*, *118*(3), 400–409. https://doi.org/10.1161/CIRCRESAHA.115.307778

Prokesch, A., Graef, F. A., Madl, T., Kahlhofer, J., Heidenreich, S., Schumann, A., Moyschewitz, E., Pristoynik, P., Blaschitz, A., Knauer, M., Muenzner, M., Bogner-Strauss, J. G., Dohr, G., Schulz, T. J., & Schupp, M. (2017). Liver p53 is stabilized upon starvation and required for amino acid catabolism and gluconeogenesis. *The FASEB Journal*, *31*(2), 732–742. https://doi.org/10.1096/fj.201600845r

Putti, R., Sica, R., Migliaccio, V., & Lionetti, L. (2015). Diet impact on mitochondrial bioenergetics and dynamics. *Frontiers in Physiology*, *6*. https://doi.org/10.3389/fphys.2015.00109

Qi, Y., Yan, L., Yu, C., Guo, X., Zhou, X., Hu, X., Huang, X., Rao, Z., Lou, Z., & Hu, J. (2016). Structures of human mitofusin 1 provide insight into mitochondrial tethering. *Journal of Cell Biology*, *215*(5), 621–629. https://doi.org/10.1083/jcb.201609019

Rahn, J. J., Stackley, K. D., & Chan, S. S. L. (2013). Opa1 Is Required for Proper Mitochondrial Metabolism in Early Development. *PLoS ONE*, *8*(3), e59218. https://doi.org/10.1371/journal.pone.0059218

Razani, B., Zhang, H., Schulze, P. C., Schilling, J. D., Verbsky, J., Lodhi, I. J., Topkara, V. K., Feng, C., Coleman, T., Kovacs, A., Kelly, D. P., Saffitz, J. E., Dorn, G. W., 2nd, Nichols, C. G., & Semenkovich, C. F. (2011). Fatty acid synthase modulates homeostatic responses to myocardial stress. *The Journal of biological chemistry*, *286*(35), 30949–30961. https://doi.org/10.1074/jbc.M111.230508

Ren, J., Zhang, N., Li, X., Sun, X., & Song, J. (2021). Identification of reference genes for gene expression studies among different developmental stages of murine hearts. *BMC Developmental Biology*, *21*(1). https://doi.org/10.1186/s12861-021-00244-6

Rodríguez-López, S., López-Bellón, S., González-Reyes, J. A., Burón, M. I., De Cabo, R., & Villalba, J. M. (2020). Mitochondrial adaptations in liver and skeletal muscle to pro-longevity nutritional and genetic interventions: The crosstalk between calorie restriction and CYB5R3 overexpression in transgenic mice. *GeroScience*, *42*(3), 977–994. https://doi.org/10.1007/s11357-020-00187-z

Rogers-Broadway, K.-R., & Karteris, E. (2015). Amplification efficiency and thermal stability of qPCR instrumentation: Current landscape and future perspectives. *Experimental and Therapeutic Medicine*, *10*(4), 1261–1264. https://doi.org/10.3892/etm.2015.2712

Roslund, K.J., Ramsey, J.J., Rutkowsky, J.M., Zhou, Z., Slupsky, C. M. (2025). Two-month ketogenic diet alters systemic and brain metabolism in middle-aged female mice. *GeroScience* 47, 935–952. https://doi.org/10.1007/s11357-024-01314-w

Rui, L. (2014). Energy Metabolism in the Liver. In R. Terjung (Hrsg.), *Comprehensive Physiology* (1. Aufl., S. 177–197). Wiley. https://doi.org/10.1002/cphy.c130024

Ruiz-Pérez, M. V., Sainero-Alcolado, L., Oliynyk, G., Matuschek, I., Balboni, N., Ubhayasekera, S. J. K. A., Snaebjornsson, M. T., Makowski, K., Aaltonen, K.,

Bexell, D., Serra, D., Nilsson, R., Bergquist, J., Schulze, A., & Arsenian-Henriksson, M. (2021). Inhibition of fatty acid synthesis induces differentiation and reduces tumor burden in childhood neuroblastoma. *iScience*, *24*(2), 102128. https://doi.org/10.1016/j.isci.2021.102128

Santel, A., Frank, S., Gaume, B., Herrler, M., Youle, R. J., & Fuller, M. T. (2003). Mitofusin-1 protein is a generally expressed mediator of mitochondrial fusion in mammalian cells. *Journal of Cell Science*, *116*(13), 2763–2774. https://doi.org/10.1242/jcs.00479

Satoh, A. (2003). Structure of the Transition State Analog of Medium-Chain Acyl-CoA Dehydrogenase. Crystallographic and Molecular Orbital Studies on the Charge-Transfer Complex of Medium-Chain Acyl-CoA Dehydrogenase with 3-Thiaoctanoyl-CoA. *Journal of Biochemistry*, *134*(2), 297–304. https://doi.org/10.1093/jb/mvg143

Schaum, N. & Tabula Muris Consortium, Overall coordination, Logistical coordination, Organ collection and processing, Library preparation and sequencing, Computational data analysis, Cell type annotation, Writing group, Supplemental text writing group, & Principal investigators (2018). Single-cell transcriptomics of 20 mouse organs creates a Tabula Muris. *Nature*, *562*(7727), 367–372. https://doi.org/10.1038/s41586-018-0590-4

Schönfeld, P., & Wojtczak, L. (2016). Short- and medium-chain fatty acids in energy metabolism: The cellular perspective. *Journal of Lipid Research*, *57*(6), 943–954. https://doi.org/10.1194/jlr.R067629

Schreurs, M., Kuipers, F., & van der Leij, F. R. (2010). Regulatory enzymes of mitochondrial beta-oxidation as targets for treatment of the metabolic syndrome. *Obesity reviews : an official journal of the International Association for the Study of Obesity*, *11*(5), 380–388. https://doi.org/10.1111/j.1467-789X.2009.00642.x

Shcherbakova, K., Schwarz, A., Apryatin, S., Karpenko, M., & Trofimov, A. (2022). Supplementation of Regular Diet With Medium-Chain Triglycerides for Procognitive Effects: A Narrative Review. *Frontiers in Nutrition*, *9*, 934497. https://doi.org/10.3389/fnut.2022.934497

Shi, B., Jiang, Y., Chen, Y., Zhao, Z., Zhou, H., Luo, Y., Hu, J., & Hickford, J. (2019). Variation in the Fatty Acid Synthase Gene (FASN) and Its Association with Milk Traits in Gannan Yaks. *Animals*, *9*(9), 613. https://doi.org/10.3390/ani9090613

Smoczek, M., Vital, M., Wedekind, D., Basic, M., Zschemisch, N.-H., Pieper, D. H., Siebert, A., Bleich, A., & Buettner, M. (2020). A combination of genetics and microbiota influences the severity of the obesity phenotype in diet-induced obesity. *Scientific Reports*, *10*(1). https://doi.org/10.1038/s41598-020-63340-w

Song, M., Franco, A., Fleischer, J. A., Zhang, L., & Dorn, G. W. (2017). Abrogating Mitochondrial Dynamics in Mouse Hearts Accelerates Mitochondrial Senescence. *Cell Metabolism*, *26*(6), 872-883.e5. https://doi.org/10.1016/j.cmet.2017.09.023

Song, M., Mihara, K., Chen, Y., Scorrano, L., & Dorn, G. W. (2015). Mitochondrial Fission and Fusion Factors Reciprocally Orchestrate Mitophagic Culling in Mouse Hearts and Cultured Fibroblasts. *Cell Metabolism*, *21*(2), 273–286. https://doi.org/10.1016/j.cmet.2014.12.011

Sternberg, F., Sternberg, C., Dunkel, A., Beikbaghban, T., Gregor, A., Szarzynski, A., Somoza, V., Walter, I., Duszka, K., Kofler, B., & Pohl, E. E. (2023). Ketogenic diets composed of long-chain and medium-chain fatty acids induce cardiac fibrosis in mice. *Molecular Metabolism*, *72*, 101711. https://doi.org/10.1016/j.molmet.2023.101711

Tamura, Y. O., Sugama, J., Iwasaki, S., Sasaki, M., Yasuno, H., Aoyama, K., Watanabe, M., Erion, D. M., & Yashiro, H. (2021). Selective Acetyl-CoA Carboxylase 1 Inhibitor Improves Hepatic Steatosis and Hepatic Fibrosis in a Preclinical Nonalcoholic Steatohepatitis Model. *The Journal of Pharmacology and Experimental Therapeutics*, *379*(3), 280–289. https://doi.org/10.1124/jpet.121.000786

Tan, B. L., & Norhaizan, M. E. (2019). Effect of High-Fat Diets on Oxidative Stress, Cellular Inflammatory Response and Cognitive Function. *Nutrients*, *11*(11), 2579. https://doi.org/10.3390/nu11112579

Tang, M., Tu, Y., Gong, Y., Yang, Q., Wang, J., Zhang, Z., Qin, J., Niu, S., Yi, J., Shang, Z., Chen, H., Tang, Y., Huang, Q., Liu, Y., Billadeau, D. D., Liu, X., Dai, L., & Jia, D. (2025). β-hydroxybutyrate facilitates mitochondrial-derived vesicle biogenesis and improves mitochondrial functions. *Molecular Cell*, *85*(7), 1395-1410.e5. https://doi.org/10.1016/j.molcel.2025.02.022

Tatsumi, K., Ohashi, K., Taminishi, S., Okano, T., Yoshioka, A., & Shima, M. (2008). Reference gene selection for real-time RT-PCR in regenerating mouse livers. *Biochemical and Biophysical Research Communications*, *374*(1), 106–110. https://doi.org/10.1016/j.bbrc.2008.06.103

Terry, A. R., & Hay, N. (2024). Emerging targets in lipid metabolism for cancer therapy. *Trends in Pharmacological Sciences*, *45*(6), 537–551. https://doi.org/10.1016/j.tips.2024.04.007

Tian, J., Goldstein, J. L., & Brown, M. S. (2016). Insulin induction of SREBP-1c in rodent liver requires LXRα-C/EBPβ complex. *Proceedings of the National Academy of Sciences*, *113*(29), 8182–8187. https://doi.org/10.1073/pnas.1608987113

Tokuyama, T., & Yanagi, S. (2023). Role of Mitochondrial Dynamics in Heart Diseases. *Genes*, *14*(10), 1876. https://doi.org/10.3390/genes14101876

Tolvanen, K. E. S., & Karp, M. T. (2011). Molecular methods for characterizing mixed microbial communities in hydrogen-fermenting systems. *International Journal of Hydrogen Energy*, *36*(9), 5280–5288. https://doi.org/10.1016/j.ijhydene.2011.01.029

Trepiana, J., Milton-Laskibar, I., Gómez-Zorita, S., Eseberri, I., González, M., Fernández-Quintela, A., & Portillo, M. P. (2018). Involvement of 5′AMP-Activated Protein Kinase (AMPK) in the Effects of Resveratrol on Liver Steatosis. *International Journal of Molecular Sciences*, *19*(11), 3473. https://doi.org/10.3390/ijms19113473

Tzec-Interián, J. A., González-Padilla, D., & Góngora-Castillo, E. B. (2025). Bioinformatics perspectives on transcriptomics: A comprehensive review of bulk and single-cell RNA sequencing analyses. *Quantitative biology (Beijing, China)*, *13*(2), e78. https://doi.org/10.1002/qub2.78

Valentin-Escalera, J., Leclerc, M., & Calon, F. (2024). High-Fat Diets in Animal Models of Alzheimer's Disease: How Can Eating Too Much Fat Increase Alzheimer's Disease Risk? *Journal of Alzheimer's Disease*, *97*(3), 977–1005. https://doi.org/10.3233/JAD-230118

Volpicella, M., Sgobba, M. N., Laera, L., Francavilla, A. L., De Luca, D. I., Guerra, L., Pierri, C. L., & De Grassi, A. (2025). Carnitine O-Acetyltransferase as a Central Player in Lipid and Branched-Chain Amino Acid Metabolism, Epigenetics, Cell Plasticity, and Organelle Function. *Biomolecules*, *15*(2), 216. https://doi.org/10.3390/biom15020216

Von Der Malsburg, A., Sapp, G. M., Zuccaro, K. E., Von Appen, A., Moss, F. R., Kalia, R., Bennett, J. A., Abriata, L. A., Dal Peraro, M., Van Der Laan, M., Frost, A., & Aydin, H. (2023). Structural mechanism of mitochondrial membrane remodelling by human OPA1. *Nature*, *620*(7976), 1101–1108. https://doi.org/10.1038/s41586-023-06441-6

Wang, H., Yu, W., Wang, Y., Wu, R., Dai, Y., Deng, Y., Wang, S., Yuan, J., & Tan, R. (2023). p53 contributes to cardiovascular diseases via mitochondria dysfunction: A new paradigm. *Free Radical Biology and Medicine*, *208*, 846–858. https://doi.org/10.1016/j.freeradbiomed.2023.09.036

Wang, Y., Mohsen, A.-W., Mihalik, S. J., Goetzman, E. S., & Vockley, J. (2010). Evidence for Physical Association of Mitochondrial Fatty Acid Oxidation and Oxidative Phosphorylation Complexes. *Journal of Biological Chemistry*, *285*(39), 29834–29841. https://doi.org/10.1074/jbc.M110.139493

Wang, Y., Yu, W., Li, S., Guo, D., He, J., & Wang, Y. (2022). Acetyl-CoA Carboxylases and Diseases. *Frontiers in Oncology*, *12*, 836058. https://doi.org/10.3389/fonc.2022.836058

Wedan, R. J., Longenecker, J. Z., & Nowinski, S. M. (2024). Mitochondrial fatty acid synthesis is an emergent central regulator of mammalian oxidative metabolism. *Cell metabolism*, *36*(1), 36–47. https://doi.org/10.1016/j.cmet.2023.11.017

Wei, S.-J., Schell, J. R., Chocron, E. S., Varmazyad, M., Xu, G., Chen, W. H., Martinez, G. M., Dong, F. F., Sreenivas, P., Trevino, R., Jiang, H., Du, Y., Saliba, A., Qian, W., Lorenzana, B., Nazarullah, A., Chang, J., Sharma, K., Munkácsy, E., … Gius, D. (2024). Ketogenic diet induces p53-dependent cellular senescence in

multiple organs. *Science Advances*, *10*(20). https://doi.org/10.1126/sciadv.ado1463

Westermann, B. (2010). Mitochondrial fusion and fission in cell life and death. *Nature Reviews Molecular Cell Biology*, *11*(12), 872–884. https://doi.org/10.1038/nrm3013

Witters, L. A., & Bacon, G. W. (1985). Protein phosphatases active on acetyl-CoA carboxylase phosphorylated by casein kinase I, casein kinase II and the cAMP-dependent protein kinase. *Biochemical and Biophysical Research Communications*, *130*(3), 1132–1138. https://doi.org/10.1016/0006-291X(85)91733-4

Wu, X., Qin, L., Fako, V., & Zhang, J.-T. (2014). Molecular mechanisms of fatty acid synthase (FASN)-mediated resistance to anti-cancer treatments. *Advances in Biological Regulation*, *54*, 214–221. https://doi.org/10.1016/j.jbior.2013.09.004

You, Y. N., Ling, P., Qu, J. Z., & Bistrian, B. R. (2008). Effects of Medium-Chain Triglycerides, Long-Chain Triglycerides, or 2-Monododecanoin on Fatty Acid Composition in the Portal Vein, Intestinal Lymph, and Systemic Circulation in Rats. *Journal of Parenteral and Enteral Nutrition*, *32*(2), 169–175. https://doi.org/10.1177/0148607108314758

Yu, R., Jin, S., Lendahl, U., Nistér, M., & Zhao, J. (2019). Human Fis1 regulates mitochondrial dynamics through inhibition of the fusion machinery. *The EMBO Journal*, *38*(8), e99748. https://doi.org/10.15252/embj.201899748

Yu, S., Go, G., & Kim, W. (2019). Medium Chain Triglyceride (MCT) Oil Affects the Immunophenotype via Reprogramming of Mitochondrial Respiration in Murine Macrophages. *Foods*, *8*(11), 553. https://doi.org/10.3390/foods8110553

Yu, S., Ji, G., & Zhang, L. (2022). The role of p53 in liver fibrosis. *Frontiers in Pharmacology*, *13*. https://doi.org/10.3389/fphar.2022.1057829

Zaman, M., & Shutt, T. E. (2022). The Role of Impaired Mitochondrial Dynamics in MFN2-Mediated Pathology. *Frontiers in Cell and Developmental Biology*, *10*, 858286. https://doi.org/10.3389/fcell.2022.858286

Zerihun, M., Sukumaran, S., & Qvit, N. (2023). The Drp1-Mediated Mitochondrial Fission Protein Interactome as an Emerging Core Player in Mitochondrial Dynamics and Cardiovascular Disease Therapy. *International journal of molecular sciences*, *24*(6), 5785. https://doi.org/10.3390/ijms24065785

Zhang, Z., Wakabayashi, N., Wakabayashi, J., Tamura, Y., Song, W.-J., Sereda, S., Clerc, P., Polster, B. M., Aja, S. M., Pletnikov, M. V., Kensler, T. W., Shirihai, O. S., Iijima, M., Hussain, M. A., & Sesaki, H. (2011). The dynamin-related GTPase Opa1 is required for glucose-stimulated ATP production in pancreatic beta cells. *Molecular Biology of the Cell*, *22*(13), 2235–2245. https://doi.org/10.1091/mbc.e10-12-0933

Zhang, Z., Zhou, Y., Mendelsohn, N. J., Bauer, G. S., & Strauss, A. W. (1997). Regulation of the human long chain acyl-CoA dehydrogenase gene by nuclear hormone receptor transcription factors. *Biochimica et Biophysica Acta (BBA) - Gene Structure and Expression*, *1350*(1), 53–64. https://doi.org/10.1016/S0167-4781(96)00141-8

Zheng, P., Ma, W., Gu, Y., Wu, H., Bian, Z., Liu, N., Yang, D., & Chen, X. (2023). High-fat diet causes mitochondrial damage and downregulation of mitofusin-2 and optic atrophy-1 in multiple organs. *Journal of Clinical Biochemistry and Nutrition*, *73*(1), 61–76. https://doi.org/10.3164/jcbn.22-73

Figures

Tables